

Naval Research Laboratory

Washington, DC 20375-6320

AD-A269 378



2



NRL/MR/5915/93-7304

**ANOMALOUS DIELECTRIC PROPERTIES OF
CARBON-BLACK FILLED ELASTOMERS**

SDTIC
ELECTE
SEP 17 1993
A D

by

Jay Burns

*Florida Institute of Technology
Melbourne, Florida 32901*

15 July 1993

93-21699



SOPH

39

d for public release; distribution unlimited.

REPORT DOCUMENTATION PAGE

Form Approved
OMB No. 0704-0188

Public reporting burden for this collection of information is estimated to average 1 hour per response, including the time for reviewing instructions, searching existing data sources, gathering and maintaining the data needed, and completing and reviewing the collection of information. Send comments regarding this burden estimate or any other aspect of this collection of information, including suggestions for reducing this burden, to Washington Headquarters Service, Directorate for Information Operations and Reports, 1215 Jefferson Davis Highway, Suite 1204, Arlington, VA 22202-4302, and to the Office of Management and Budget, Paperwork Reduction Project (0704-0188), Washington, DC 20503.

1. AGENCY USE ONLY (Leave blank)		2. REPORT DATE 15 July 1993	3. REPORT TYPE AND DATES COVERED FINAL	
4. TITLE AND SUBTITLE Anomalous Dielectric Properties of Carbon-Black Filled Elastomers			5. FUNDING NUMBERS C - N62190-91-M-0526 PE- 61153N TA - LR011 WU - DN280-003	
6. AUTHOR(S) Jay Burns			8. PERFORMING ORGANIZATION REPORT NUMBER	
7. PERFORMING ORGANIZATION NAME(S) AND ADDRESS(ES) Jay Burns Scientific Consulting 2261 Sand Pine Road North Indiatlantic, FL 32903			10. SPONSORING/MONITORING AGENCY REPORT NUMBER NRL Memorandum Report 7304	
9. SPONSORING/MONITORING AGENCY NAME(S) AND ADDRESS(ES) NAVAL RESEARCH LABORATORY Underwater Sound Reference Detachment P.O. Box 568337 Orlando, FL 32856-8337			11. SUPPLEMENTARY NOTES	
12a. DISTRIBUTION/AVAILABILITY STATEMENT Approved for public release; distribution unlimited.			12b. DISTRIBUTION CODE	
13. ABSTRACT (Maximum 200 words) Dielectric measurements covering nearly ten decades in frequency are given for a series of neoprene elastomers containing various amounts of conductive carbon black filler. The influence of the conductive filler upon the dielectric properties of the elastomers is treated by an extension of the Maxwell-Wagner-Sillars effect to account for slow tunneling and hopping modes of conduction within the elastomer. Effects upon dielectric response due to clustering and agglomeration of carbon particles are discussed together with some of the problems associated with application of dielectric measurements to obtain information about the internal structure of inhomogeneous materials.				
14. SUBJECT TERMS Dielectric spectroscopy Carbon-black filled elastomers Maxwell-Wagner-Sillars effect Delayed dielectric relaxation			15. NUMBER OF PAGES 47	
			16. PRICE CODE	
17. SECURITY CLASSIFICATION OF REPORT UNCLASSIFIED	18. SECURITY CLASSIFICATION OF THIS PAGE UNCLASSIFIED	19. SECURITY CLASSIFICATION OF ABSTRACT UNCLASSIFIED	20. LIMITATION OF ABSTRACT UL	

BLANK PAGE

CONTENTS

INTRODUCTION	1
THEORY	4
Maxwell's Analysis	4
Time Dependence	10
Frequency Dependence	11
Geometric Effects	13
Magnitude of MWS Effects	17
Dynamics of Delayed Conduction Relaxation	22
Dispersive Transport Effects	24
Summary of Theoretical Status	26
EXPERIMENT	28
RESULTS AND DISCUSSION	31
CONCLUSIONS	40
ACKNOWLEDGEMENTS	42
REFERENCES	42

DTIC QUALITY INSPECTED

Accession For	
NTIS - GRA&I	<input checked="" type="checkbox"/>
EDS - TAC	<input type="checkbox"/>
Unannounced	<input type="checkbox"/>
Justification	
By	
Distribution	
Availability Status	
Dist	Availability Status
A-1	

BLANK PAGE

ANOMALOUS DIELECTRIC PROPERTIES OF CARBON-BLACK FILLED ELASTOMERS

INTRODUCTION

For a long time, it has been recognized that the dielectric and dynamic elastic properties of elastomeric solids are related. This follows from the modern model of an elastic polymer as a "cooked spaghetti" aggregate of long flexible chains of monomeric units, each unit having an electric dipole moment. The orientations of these dipoles in an externally applied electric field depend to some extent upon the orientations of the chain segments to which they belong; the dipoles are not entirely free to rotate but are under some constraint to rotate into certain positions with respect to their neighbors and to the axis of their parent monomer segment. In this fashion, the dipole motions are coupled to the orientational motions of their parent chain segments which are in turn responsive to applied mechanical forces. Thus, in a rather complex manner the electric dipoles move in response to elastic strains, and dielectric properties should be coupled in some way to elastic properties.

The connection between dielectric and elastic characteristics of elastomers has been studied both theoretically and experimentally since the early 1950s and has given rise to a sizable literature and to a subfield often termed dielectric spectroscopy, though that term includes more than just the study of elasticity by dielectric measurements. Perhaps the most extensive coverage of work up to the middle 1960s has been by McCrum, Read, and Williams [1] who surveyed both the experimental and theoretical state of the field as it stood at that time. The theoretical foundations were treated in more detail by Eirshstein and Ptitsyn [2] in an extension to dielectric phenomena of theoretical work on polymer chain configurations by Volkenstein [3]. More recent surveys are by Hedvig [4] and Perepechko [5]. The most modern ideas on dielectric aspects of elastomeric polymers have been summarized by Böttcher and Bordewijk [6]. No attempt will be made here to provide an extensive coverage of the relevant literature since the references cited above thoroughly accomplish that task. Only those papers will be cited that have particular importance for understanding the special aspects of the subject to be covered in this report.

The first treatment of dielectric effects in inhomogeneous materials was given a century ago by J. C. Maxwell [7]. He considered the simplest possible case of a parallel plate condenser containing two or more layers of lossy, semiconducting dielectric material, each layer having different static dielectric constants and conductivities. Maxwell showed that, at the interfaces between different dielectrics, mobile charges (the unbound conduction electrons) could accumulate and build up charged layers giving rise to very large dipole moments. These large moments create, in effect, abnormally high dielectric constants or permittivities in such inhomogeneous material systems.

This simple model gives a clear example of how the mobile charge can contribute to the more familiar sources of dielectric polarization such as the rotational alignment of atomic-scale dipoles. In Maxwell's model massive dipoles are induced on a much larger macroscopic scale by charge transport in the semiconductive dielectric materials, blocked, or at least retarded, at interfaces within the material.

From Maxwell's model it is easy to show that under suitable conditions, which are not difficult to realize, dipole moments of the conduction electrons can overwhelm contributions due to rotation of the ordinary permanent dipoles to give very large static dielectric constants. It should be pointed out that Maxwell's model was essentially a static one though he dealt with initial and long time equilibrium states of the inhomogeneous dielectric under the application of a step function potential. He did not treat the dynamic features of intermediate states related to time-dependent formation and relaxation of the large conduction dipoles.

Little attention was paid to Maxwell's result for more than two decades until Karl Wagner [8] undertook to expand upon the essential features of Maxwell's model by considering a more interesting and practical case -- that of small spherical conducting particles embedded in a normal, non-conducting dielectric medium. Spherical particles were chosen to make it simpler to calculate the electric fields within a particle. Wagner's results confirmed the main features of Maxwell's model and showed that, in general, any inhomogeneity within a solid dielectric with mobile charge transport could give rise to large permittivities. He showed that the shape of the interface modified the phenomena somewhat but not in an essential way. Wagner also went a step further and treated the losses associated with resistance of the conduction electrons in his particles.

It remained for Sillars [9] to give a more general treatment for conducting inclusions having shapes other than spherical. He chose to treat ellipsoidal particles with varying eccentricities so he could deal with needle-like particles at one extreme and nearly flat platelets at the other. His results for spheroids agreed with those of Wagner, but Sillars was able to show more clearly how the shapes of the particles affected the overall permittivity and losses. For example, he showed that a very small amount of conducting impurity in the form of fine needles could produce serious low frequency losses, whereas the same quantity of impurity dispersed as small spheres would produce relatively little effect.

In the Theory section to follow, a more detailed discussion of both Wagner's and Sillars' results will be given together with a general treatment of the complex dielectric permittivity in the presence of both conventional dipole rotation and dispersive or delayed conduction. Both hopping and tunneling types of conduction as well as conventional, prompt ohmic conduction will be considered. The treatment will show how slow or delayed conduction may be associated with dipole rotation response.

Delayed conduction introduces a phase shift in the dynamic response, so part of the conduction current lags the applied field by 90° and this quadrature component modifies the ordinary dielectric response. The quadrature part of the conduction current contributes to the macroscopic overall dielectric permittivity. The prompt or in-phase part of the conduction and the lossy part of the complex permittivity also combine to give the overall dielectric loss and, again, there is a contribution from the conduction current. Since there are four rather than two phenomena operating in such cases, and since each has a different frequency dependence, the combined dielectric response can be much more complex than for the simple dipole rotation case.

Unconventional dielectric behavior is introduced by conduction within a heterogeneous sample. It arises, in a sense, from the usual distinction between displacement and conduction currents. Both come from charge motion, but displacement current involves localized charge motion in which the charges remain tied to their "home" ions, while conduction ordinarily refers to charges that are able to move freely through the interior of the dielectric material to the exterior circuit outside of the material itself.

In the present treatment, we use the term *conduction* to refer to electrons that may or may not reach the exterior circuit but which can move within the dielectric beyond the influence of the ion from which they originate. They are therefore not bound in the sense of an electron in a permanent dipole but are somewhat free to migrate over much larger than atomic distances within the solid. They may be subsequently trapped or otherwise prevented from moving all the way through the solid, but they can move macroscopic distances -- in contrast to the dipolar charges which remain bound to their parent ions.

Maxwell treated both conduction and dipolar or displacement currents as dynamically equivalent inasmuch as they are both sources of magnetic fields. Those "bound charges" that move only slightly (order of atomic dimensions) under the influence of an applied electric field constitute the ordinary dipoles that contribute to what is usually regarded as the dielectric constant or permittivity. In the conventional form of Maxwell's equations ($\text{curl } H = \partial D / \partial t + J$) those charges that do not leave the dielectric material are included in the displacement current term $\partial D / \partial t$, and the current per unit area that traverses the entire sample is J . However, the charge that moves but is subsequently trapped at an impurity or inhomogeneity or blocked at an interface between two inhomogeneous regions in the dielectric material must also be considered part of the displacement current.

These distinctions between the two types of currents are evidently rather artificial, and it will later be shown that it is often more convenient in dealing with periodic applied voltages to categorize currents by their phase relations to the applied voltage. Thus J includes all currents that are in phase with the applied voltage, leading to losses, while D includes all charge displacements that give quadrature currents 90° out of phase with the voltage and constitutes stored energy that is returnable to the system.

In inhomogeneous materials a whole new range of features of the generalized displacement current may arise due to the additional parameters presented by the various kinds of internal conduction processes that can take place, subject only to the condition that they be blocked or slowed in passage somewhere in the material so as not to join the conventional conduction current that moves in phase with the applied voltage.

Two important phenomenological consequences are expected to result from the limited mobility of conduction charges. First, the blocked or slowed internal conduction currents may give rise to very large dipole moments because of the macroscopic distances through which they can move before being blocked or trapped temporarily. This can lead to very high static or low frequency dielectric constants if the amount of such charge that moves is appreciable.

Second, the relatively long and varied time scales associated with the movement and trapping of the "slow" mobile charges should lead to a variety of dynamic effects that show up in measurements of the dynamic behavior of the complex permittivity. It is therefore possible to take advantage of this connection between observed dynamic dielectric properties and the internal structure of the inhomogeneous dielectric to probe internal conduction by a form of dielectric spectroscopy different from that generally used to study conventional dipolar effects. It is evident that if the time scales for the latter are considerably different from those of the former, as often proves to be the case, it becomes possible in principle to separate the two classes of effects and study them independently.

One objective of this report is to develop the connection between experiment and theory of the generalized Maxwell-Wagner-Sillars (MWS) effect embodied in the frustrated and delayed conduction mechanisms described above and to use these connections to interpret results of measurements on carbon-black filled elastomers.

THEORY

Maxwell's Analysis

The simple model analyzed by Maxwell [7] will be considered first to show the basic mechanism of enhancement of the dielectric permittivity ϵ' in a parallel plate configuration containing

at least two different dielectric materials, each having some electrical conductivity. In what follows the complex permittivity or dielectric "constant" will be designated ϵ^* with the superscript * referring generally to a complex quantity. In the case of ϵ^* , the real and imaginary parts will be ϵ' and ϵ'' , respectively, and the sign convention is shown by the form

$$\epsilon^* = \epsilon' - j\epsilon'' \tag{1}$$

with $j = \sqrt{-1}$.

Maxwell considered the total time dependent current flow in a multilayered conducting dielectric system. Only the storage permittivity ϵ' is obtained from his model. Maxwell's treatment can be considerably condensed as follows:

Consider a parallel plate capacitor of unit area as shown in Fig. 1, having two or more layers of dielectric. Let the i^{th} layer have permittivity ϵ_i , resistivity ρ_i , and thickness a_i . The total current density in the i^{th} layer, including both displacement and conduction currents, will be given by the Maxwell equation

$$(\nabla \times H)_i = \left(\frac{\partial D}{\partial t} \right)_i + J_i = J_i \tag{2}$$

where $(\partial D/\partial t)_i$ is the displacement current, and J_i is the conduction current normal to the layer, both in layer i . Since in this planar configuration there is no current parallel to the layer within a layer or at an interface, the left hand term in Eq. (2) is a constant equal to the total current J_i , consisting of both displacement and conduction currents in the i^{th} layer. The total current is the same in every layer and through every interface, since all layers and interfaces are in series, and is the current delivered by the external source.

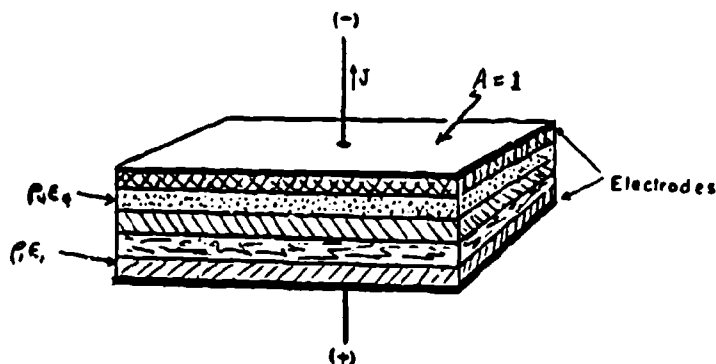


Fig. 1 - Schematic arrangement of Maxwell's parallel plate capacitor model of an inhomogeneous dielectric.

At long times after application of an external voltage V_0 , the system will approach a steady state in which all $\partial D/\partial t$ go to zero and the total current will consist of conduction current only. At this point all of the J_i will be equal and will equal the total current $J_t = V_0/R$, where the total resistance $R = \sum \rho_i a_i$. Prior to attainment of steady state, the individual fields on either side of an interface and the conduction currents J_i adjust themselves in accordance with the material parameters ρ and ϵ to maintain the same total current in each layer. Therefore, if D changes from one layer to the next because ϵ and ρ differ in the two layers, $\partial D/\partial t$ and J in each layer must change to compensate. Surface charges of density σ will accumulate at the interface causing J to change, as required, by a readjustment of the local electric field in the layer. The resulting surface charges are equivalent to charges of opposite sign separated by the thickness of the layer, and they form large electric dipoles of magnitude proportional to the product of surface charge density times the layer thickness.

The equilibrium surface charge density at an interface is proportional to the total current J_t times the difference in products of permittivity and resistivity on opposite sides of the interface. Thus the magnitude of the "conductivity dipole moment" depends upon layer thickness, the difference in layer conductivities, the change in ϵ across the interface, and the total conduction current J_t .

Quantitatively, if a capacitor containing a layered dielectric is connected to a voltage source, the source voltage V_0 will be the sum of voltages across each layer. Dynamically, the buildup of surface charge upon application of the external voltage is not instantaneous. It takes time for the permanent dipoles to reorient in the applied field and generally different time for the mobile conduction charge to migrate across a dielectric layer to form the surface charge at the interface. Maxwell calculated these times for a given layer in terms of a characteristic time constant $\rho\epsilon$ for the material of that layer.

[Note that SI units will be used throughout unless otherwise stated, and all permittivities ϵ' and ϵ'' are assumed to be absolute values; i.e., relative permittivities multiplied by ϵ_0 , the permittivity of free space. To simplify the notation whenever it is unnecessary to distinguish between ϵ' and ϵ'' , the permittivity will be designated simply by ϵ .]

Maxwell's treatment may be paraphrased by considering the situation in the first layer of a system of unit area. Ohm's law gives for the conduction part of the total current $E_1 = \rho_1 J_1 = V_1/a_1$, where E_1 is the electric field in layer 1, and V_1 is the voltage across the layer of thickness a_1 . E , V , and J are all functions of time. The displacement part of the current is $(\partial D/\partial t)_1$, where D is the usual electric displacement related to the dipole moment per unit volume P , as usual, by $D = \epsilon_0 E + P$.

The displacement D undergoes a discontinuity $\sigma_{12} = D_2 - D_1$ at the interface between layers 1 and 2, and σ_{12} is the surface charge density responsible for this discontinuity. The surface charge

may be determined from $\partial\sigma_{12}/\partial t = \partial D_2/\partial t - J_2 - J_1$, which is just another way of saying that $\nabla \times H$ (or the total current) is continuous across an interface. Making use of $D_i = \epsilon_i E_i$ and $J_i = E_i/\rho_i$, Eq. (2) may be written in terms of E_i as

$$J_i = \frac{E_i}{\rho_i} + \frac{\epsilon_i \partial E_i}{\partial t} . \quad (3)$$

This equation has solutions of familiar exponential form, $E_i(t) = E_i(0) \exp(-t/\rho_i \epsilon_i)$, so there is in each layer an exponential response with individual time constants, $\tau_i = \rho_i \epsilon_i$. The layered system behaves like a set of resistor-capacitor units connected in series, each with its own time constant.

The sudden application of an external voltage V_o to an uncharged system of this kind places an initial field $E_i(0) = Q/\epsilon_i$ on the i^{th} layer (by voltage divider action), where Q is the total charge delivered by the voltage source. Therefore, the source voltage $V_o = Q \sum a_i/\epsilon_i$ and the overall capacitance will be $C = [\sum a_i/\epsilon_i]^{-1}$, the same result as would be obtained neglecting the conductivity of the layers.

After a long time the system reaches steady state in which the layer resistivities determine the voltages across each layer, and $V_o = J_i \sum \rho_i a_i = R J_i$, where R is the total series resistance of the system. In this state the field across the i^{th} layer is

$$E_i = \rho_i J_i . \quad (4)$$

The displacement in the i^{th} layer then becomes

$$D_i = \epsilon_i E_i = \rho_i \epsilon_i J_i . \quad (5)$$

Therefore, the interfacial charge density σ_{12} at the first interface between layers 1 and 2 will be

$$\sigma_{12} = (\rho_2 \epsilon_2 - \rho_1 \epsilon_1) J_1 . \quad (6)$$

This equation gives the magnitude of the final interfacial accumulated space charge density in terms of the change in characteristic time constants $\tau_i = \rho_i \epsilon_i$, so Eq. (6) may be rewritten simply as

$$\sigma_{12} = (\tau_2 - \tau_1) J_1 . \quad (7)$$

A similar expression may be written for the i^{th} interface.

The dipole moment p_i developed in layer 1 by charge transfer that produces σ_{12} from a layer of thickness a_1 will be $\frac{1}{2} a_1 \sigma_{12}$, the factor $\frac{1}{2}$ coming from the fact that on average the charge σ_{12} has

moved only half the thickness of the layer, while the positive charges remain fixed in the solid lattice. In general the i^{th} layer will contribute a dipole moment

$$p_i = \frac{1}{2} a_i (\tau_{i+1} - \tau_i) J_i . \quad (8)$$

Its "normal" permittivity is therefore enhanced by addition of the conductive dipole moments p_i given by Eq. (8).

It may be seen that enhancement by conduction dipoles appears only if there is a variation in τ between layers, and the magnitude of the effect is proportional to the product of layer thickness, the total steady state current density J_i , and the differences in τ across the interfaces. For macroscopic values of a_i , even small variations in τJ in an inhomogeneous medium can give rise to relatively large net static permittivities ϵ . Note, also, that the dipole moment is proportional to the ohmic current density J_i , so conduction polarization contributes significantly to the effective permittivity only if the materials have relatively high conductivities or sufficiently high applied voltages to give appreciable values of J . This, then, is the origin of the MWS effect.

A special case is often encountered, when there is a single layer of conductive dielectric bounded by highly conducting electrodes, or alternatively with a very thin, low conductivity film of oxide or air interposed between dielectric and electrodes. The relevant interfaces here are at the electrode surfaces where they may give rise to macroscopic dipole moments. In this case the resulting MWS effect is often referred to as the "electrode effect".

The conductive contribution to the total dipole moment, given by Eq. (8), takes time to become fully established, and this time dependence can also be found for Maxwell's simple model. Within a given dielectric layer two related processes take place upon application of an external voltage: ohmic conduction begins, and permanent dipole orientation also commences. As polarization by orientation of the permanent dipoles proceeds, the effective local electric field seen by the conduction electrons decreases due to buildup of an opposing, depolarizing field that acts to slow conduction. A depolarizing field also arises from charge trapped at interfaces, i.e., from the buildup of conduction dipoles. Again, this slows conduction and affects the dynamics of the process. Therefore, the two polarization processes are not independent. The problem may be restated more simply: as charges move under the application of the external field, the interior field begins to weaken as soon as the system responds, and the weakened field slows the further response of the system. The net result in the simpler case of pure dipole rotation response (no conduction) was worked out long ago by Debye [10], Fröhlich [11], and others. However, in the presence of conductive particles the problem is more complex. We will not consider the general case but will assume that one process, either dipole rotation or formation of conduction dipole moments, is much faster than the other. This is often the case and seems to be true in the elastomers studied in the present work where the 5109 neoprenes

used appear to have their principal dielectric losses, those attributable to dipole rotation, in the megahertz region of the spectrum. These are the so-called α -loss peaks.

In carbon filled rubber, the carbon particles themselves have resistivities of the order of $4000 \mu\Omega\text{-cm}$. The characteristic time constant $\tau = \rho\epsilon$ of these particles is of the order of 10^{-14} second, which would produce observable effects in the optical middle infra-red region of the spectrum.

Other conduction mechanisms such as hopping and tunneling between carbon particles give very much higher resistivities sufficient to produce long time constants that can lead to loss peaks at quite low frequencies. For example, resistivities of order $5 \times 10^{11} \Omega\text{-cm}$ are found at room temperature in neoprenes with less than about 20% carbon black by weight. The time constant for such samples is of the order of five seconds, giving loss peaks near 1 Hz. The conduction polarization is small in such samples as long as the current density is low, as it is when the applied field is kept small to avoid non-linear effects. Typically the applied field in our work was less than $\frac{1}{2}$ volt/cm, giving $J = 10^{-12}$ A/cm² and a conduction dipole moment density of $\sim 10^{12}$ coulomb-cm². This dipole moment is about 0.1 Debye unit per monomer molecule (1 Debye unit = 10^{-18} esu-cm or $\frac{1}{2} \times 10^{-27}$ coulomb-cm). Therefore, the conduction dipoles in these high resistivity materials contribute an amount comparable to or less than the ordinary dipole rotation to the overall permittivity, i.e., the MWS effect is present but not dominant.

Conduction permittivity will be roughly proportional to the carbon black content of the material in the range under about 20% carbon, but the loss peak due to free charge motion will not be pronounced at these carbon concentrations and may be obscured by the $1/f$ feature at low frequencies to be discussed later.

When the carbon content increases above about 20% there is a rapid decrease in resistivity with concentration (see Fig. 2). This is believed to be due to carbon agglomerates becoming large enough to form continuous percolation-type conduction paths through the entire sample. As Fig. 2 shows, ρ decreases to about $10^9 \Omega\text{-cm}$ beyond this percolation threshold. The value of τ therefore increases by several orders of magnitude, reducing the loss peak frequency to the milli-Hertz region or lower and giving rise to the electrode effect mentioned earlier. Such ultralow frequency effects tend to be large in magnitude because dipoles associated with them are macroscopic, the charge transport being across the full thickness of the sample. In addition, beyond the percolation threshold the current density J , increases considerably for the same applied voltage, further enhancing the magnitudes of the conduction dipoles.

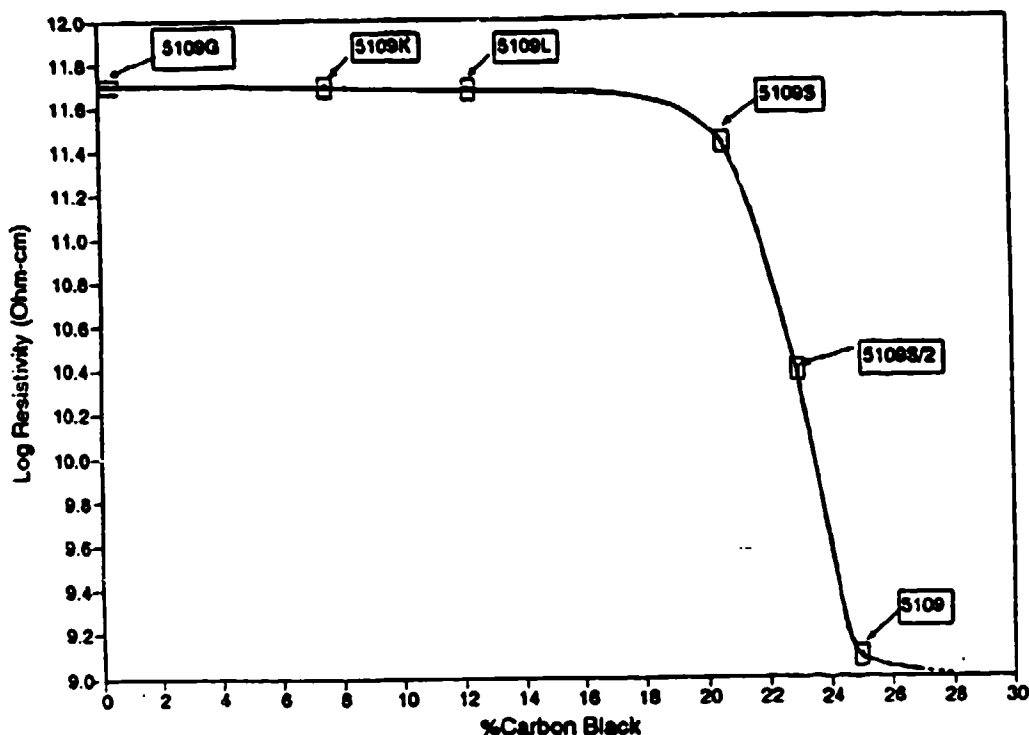


Fig. 2 - DC resistivity vs carbon black content for a series of 5109-type neoprenes measured at 27°C.

Time Dependence

When dipole rotation response is much faster than the response of conduction dipoles, the effective local field for the conduction process is the applied field already fully reduced by the equilibrium depolarizing field of the dipole rotation. The net reduction in field by depolarization through dipole rotation depends upon the geometry of the system. In the simple parallel plate case the depolarizing factor is simply $1/\epsilon_d$, where ϵ_d is the part of the permittivity contributed by dipole rotation, which is not very large for materials with relatively low static permittivities, as in the materials under study here. The conclusion is that once the dipole response is complete, the subsequent conduction process and buildup of conduction dipoles takes place under an interior field that is E_{app}/ϵ_d . This is a reduced field but not drastically reduced, the reduction factor ϵ_d being roughly 3-6.

Conduction electrons do not move in a constant field because, as the conduction polarization builds up, it also produces a counterfield that slows conduction. Therefore, the conduction electrons move under a time-varying local field. The resultant polarization produced by movement of these electrons toward an interface is therefore not a simple exponential function of t/τ , as might be expected. Here, $\tau = \rho\epsilon$ is itself time-dependent, at least through the time dependence of $\epsilon(t)$ and in some cases from a time dependence in ρ , as well. It is evident that the process is inherently nonlinear: σ_{12} will be proportional to a factor $(1 - \exp[-t/\tau(t)])$, and the dipole field in layer 1 will be

proportional to $a_1 \sigma_{12}$. Since $\epsilon(t)$ is proportional to the dipole field, we would expect to find $\epsilon(t)$ a function of $(1 - \exp[-bt/\epsilon(t)])$, making the problem clearly nonlinear. Only for times long enough that the exponential term is negligible does the nonlinearity vanish, with ϵ approaching a constant limiting value. At short times, expansion of the exponential term gives a quadratic and higher order expression for $\epsilon(t)$, so the nonlinearity remains at the short end of the conduction polarization time scale. This matter seems to have been overlooked in the literature on the MWS effect, so its ramifications have not yet been explored.

Qualitatively the effect of the nonlinearity can be seen by noting that as time goes on after application of an external electric field, the local internal field decreases as the depolarizing field grows. This leads to a reduction in conduction current J_i below what it would otherwise be. The net effect is to lengthen the time for charging the interface, i.e., for formation of σ_{12} . The time constant for conductive charging τ_c is thus increased, and the increase is progressive in the sense that as the interface charges, τ_c becomes longer and longer. This leads to something akin to the "long-tailed" or stretched-exponential response typical of dispersive transport [12,13]. Experimentally we find something like a stretched exponential character in the very low frequency dielectric response in carbon-filled neoprene elastomers.

The nonlinearity in time development of $\epsilon(t)$ leads to an integral equation. Instead of attempting to solve it, even approximately or numerically, a more conventional, empirical approach will be taken. The response will be assumed to be a superposition of time-delayed responses in the form commonly used in hereditary mechanics based upon the fading memory principle [14-16]. The response $v(t)$ to a force u is the cumulative sum (integral) of all earlier values of $u(t, \tau)$ where $t > 0$ and $0 \leq \tau \leq t$. Each earlier force is modified by the fading memory function $G(t, \tau)$ acting over the intervening interval $(t - \tau)$. The form is thus

$$v(t) = v(0) + \int_0^t G(t, \tau) u(\tau) d\tau \quad (9)$$

The fading memory function is usually taken as a decreasing exponential of the form $\exp(-t/\tau)$. This form has the practical virtue of making the integral in Eq. (9) a Laplace transform of the force function u which greatly facilitates further mathematical manipulation. However, as already noted, the nonlinearity of the problem spoils the simple exponential time decay, so the memory function is expected to have a more complicated form. Moreover, the superposition principle is not generally applicable in nonlinear problems, leaving one at a loss to know even how to set up the problem. In such cases it has been the practice to ignore the latter difficulty and to treat the problem in a quasi linear manner, at least to the extent of using superposition and its basic formulation in the form of Eq. (9). The function $G(t, \tau)$ is then determined empirically from the measured response to a simple forcing function such as a voltage step function or a sinusoidal applied voltage. It is found in many cases and in many diverse phenomena [13] that $G(t, \tau)$ can be fitted rather well by a "stretched exponential" function of the form

$$G(t, \tau) = A \exp \left[-b \left(\frac{t}{\tau} \right)^\beta \right], \quad (10)$$

where A , b , and β are constant parameters. Scher, et al, [12] have shown that this form leads to the "long-tailed" anomalous dispersive transport observed in the form of a $t^{-(1+\beta)}$ dependence of the transport flux which in our case is the conduction current that leads to internal charge buildup at interfaces $\sigma_{i,i+1}$.

Qualitatively, at least, the above procedure gives a sensible result; namely, an anomalously long decay time for the response to an applied force, which in the present case is internal current flow under applied external field. This is consistent with the earlier expectation that response times would be lengthened by reduction in the internal electric field due to buildup of macroscopic dipoles by trapping of charge σ_i at interfaces. Whether there is quantitative agreement with the stretched exponential memory function remains to be determined by a more systematic analysis. However, we shall proceed using the superposition formulation embodied in Eqs. (9) and (10).

Frequency Dependence

Up to this point no explicit mention has been made of the frequency response to an applied alternating field. Formally, a Fourier transform of the time domain response gives the frequency response. However, the conventional method of arriving at the frequency response is to sum the responses of all the oscillating dipoles of every kind with appropriate weighting for each. The weighting function is, of course, unknown a priori, so it is regarded as a fitting function to be determined from experiment.

The response of a rotating dipole with a relaxation time constant τ to a sinusoidal electric field of circular frequency ω was found by Debye [10] (also see ref. [11]).

The form is simple:

$$\epsilon^*(\omega) = \epsilon_\infty + \frac{\epsilon_s - \epsilon_\infty}{1 - j\omega\tau} \quad (11)$$

Separation of real and imaginary parts gives

$$\epsilon'(\omega) = \epsilon_\infty + \frac{\epsilon_s - \epsilon_\infty}{1 + \omega^2\tau^2} \quad (12)$$

and

$$\epsilon''(\omega) = \frac{(\epsilon_s - \epsilon_\infty)\omega\tau}{1 + \omega^2\tau^2}, \quad (13)$$

where ϵ_s is the static or low frequency limiting value of ϵ' , and ϵ_∞ is its high frequency limiting value.

These Debye equations are used for a wide variety of relaxation processes in physics even when the relaxation mechanisms may be quite different from the simple dipole model for which it was derived. There is, however, a justification for this. The Debye functions form a continuous, complete orthogonal set with respect to either ω or τ , so any reasonably well-behaved function can be expanded in Debye functions to give an integral equation representation of the function similar to the Fourier integral representation. Thus, in general

$$\epsilon''(\omega) = N \int_0^\infty g(\tau) D(\omega\tau) d\tau, \quad (14)$$

where $D(\omega\tau)$ is the Debye function, Eq (11), and $g(\tau)$ is the weighting function or distribution function for response times τ . The generality of this representation makes it useful aside from any questions as to the "correctness" of the Debye function for a given relaxation mechanism. Of course, if $D(\omega\tau)$ does not properly represent the relaxation mechanism, then the distribution function $g(\tau)$ may not have much physical meaning itself, being more in the nature of a curve fitting function. In any event, Eq. (14) will be taken as the basis for the dynamic treatment in this report.

Temperature enters the dynamic picture primarily through the τ 's in $g(\tau)$ and to a much smaller extent through ϵ_s and ϵ_∞ . The τ dependence on temperature is approximately exponential in a semiconducting material and is evident experimentally through the frequency shift of a given point on the $\epsilon'(\omega)$ and $\epsilon''(\omega)$ curves [e.g., the loss peak in $\epsilon''(\omega)$] as temperature changes. The loss peak for a single relaxation time process occurs, for example, at $\omega\tau=1$ so the frequency of the peak ω_p shifts inversely with τ as temperature T changes. On the customary logarithmic frequency scale the loss peak would shift as $(-1/T)$, shifting to lower frequency as T goes down.

However, if the more conductive phase in a composite dielectric is a metal or semimetal, the temperature dependence of τ is not so pronounced and may in fact be very small in the case of a metal. In the filled elastomers considered here the conductive phase consists of colloidal carbon particles or aggregates, and these possess a small negative temperature coefficient of resistivity, giving rise to a small loss peak shift in the same direction as temperature moves, i.e., to lower frequency as T goes down. This is what is observed experimentally.

The relative permittivity ϵ of carbon in diamond form is about 5.7 [17]. The values for graphite and amorphous forms will be somewhat less. The resistivity of graphite is about $1400 \mu\Omega\text{-cm}$ and for amorphous carbon is about $4000 \mu\Omega\text{-cm}$. Therefore, the time constant $\tau = \rho\epsilon$ lies in the 10^{-14} second range, as pointed out earlier.

It is quite probable that the carbon is in the form of loose, dendritic aggregates. In this case, the resistivity of the particulates will be much larger than the values cited, which apply to compact, single carbon particles. Conduction within a particulate may well involve hopping and tunneling between individual carbon particles that make up the particulate. Such conduction mechanisms are common in amorphous materials. They can be quite slow and variable, and they often depend strongly upon temperature, as well.

The sort of hopping or tunneling conduction that is typical of charge transfer in amorphous materials frequently exhibits the fractional- or stretched-exponential response mentioned earlier, leading to a long-tailed algebraic, rather than exponential, decline in conduction with time. This slow decline makes the loss peak asymmetric on a log frequency scale with the low frequency side of the peak trailing off slowly toward lower frequencies while the high frequency side has a normal bell-shaped form. Such asymmetry, if it can be seen at all in the presence of the rising $1/f$ characteristic of dc conduction of the system, is a good clue to the presence of hopping/tunneling conduction and indirectly points to loose aggregate forms of the carbon particulates.

Geometric Effects

So far, the discussion of the dynamic character of the MWS effect has been in general terms based on Debye-Fröhlich theory. It should be evident that the shapes of the conductive particles or aggregates play an important role in the MWS effect. This is because the electric field seen by the mobile charge within a particle is a function of its shape. From a macroscopic point of view the field equations, Laplace or Poisson, must satisfy appropriate boundary conditions at the interfacial surface of a semiconducting particle inside the material. The shape of the interface is therefore important; so is its orientation with respect to the internal field. Thus, there are two parameters to be considered: both particle shape and orientation with respect to the field.

The simplest case, dealing with spherical conducting particles, was treated by Wagner [8]. His result can be put into the following form [9]:

$$\epsilon' = \epsilon_{\infty} \left[1 + \frac{K}{1 + (\omega\tau)^2} \right] \quad (15)$$

and

$$\epsilon'' = \epsilon_{\infty} \frac{K\omega\tau}{1 + (\omega\tau)^2}, \quad (16)$$

where

$$\epsilon_{\infty} = \epsilon'_1 \left[1 + \frac{3q(\epsilon'_2 - \epsilon'_1)}{2\epsilon'_1 + \epsilon'_2} \right], \quad (17)$$

$$K = \frac{9q\epsilon'_2}{2\epsilon'_1 + \epsilon'_2}, \quad (18)$$

and

$$\tau = (2\epsilon'_1 + \epsilon'_2)\rho_2. \quad (19)$$

The permittivities ϵ'_1 and ϵ'_2 are the real part of ϵ^* for the insulating and conductive media respectively, q is proportional to the concentration of conducting material, and ρ_2 is the resistivity of the conducting particles.

The form of Eqs. (15) and (16) is just that of the Debye-Fröhlich dynamical theory, as would be expected, with K being a shape factor having the specific form given in Eq. (18) for the special case of spherical conducting particles. K comes from a solution of the electrostatic field problem that satisfies the boundary conditions on a sphere of conductivity ρ_2 and dielectric permittivity ϵ'_2 surrounded by an infinite insulating medium of dielectric constant ϵ'_1 . Rewriting Eq. (14) in expanded form gives

$$\epsilon' = \epsilon_{\infty} \left[1 + \int_0^{\infty} g(\tau) \frac{1}{1 + (\omega\tau)^2} d\tau \right], \quad (20)$$

$$\epsilon'' = \epsilon_{\infty} \int_0^{\infty} g(\tau) \frac{\omega\tau}{1 + (\omega\tau)^2} d\tau. \quad (21)$$

Wagner assumed the logarithms of the resistivities of the individual particles to be distributed in a Gaussian fashion about the mean value. This will be recognized as a log-normal distribution. From this assumption, the form of $g(\tau)$ can be written immediately as

$$g(\tau) = \frac{q}{\sqrt{2\pi} \sigma \tau} \exp \left[-\frac{[\log(\tau/\tau_0)]^2}{2\sigma^2} \right], \quad (22)$$

where, as before, q is proportional to the concentration of conductive material present, and τ_0 is the time constant associated with the mean value of the resistivity. The parameter σ , as usual, a measure of the width of the distribution and is to be regarded as a parameter that is found in practice by curve fitting to the shape of an experimental curve of ϵ'' vs log frequency. It is not clear whether the choice of a log-normal distribution was considered by Wagner to have any particular physical significance or whether its choice was simply a matter of mathematical convenience in view of the fact that experimental curves of ϵ'' plotted on a log frequency scale are more or less symmetrical and generally bell-shaped of Gaussian form. The latter seems the more likely.

Yager [18] has given a rather extensive discussion of relaxation time distributions in dielectrics and has shown that the log-normal distribution is consistent with a superposition of exponentially decaying response functions. Each such exponential response function generates a Debye-type frequency response of the form in Eq. (14), the weighted sum of which gives Eqs. (20) and (21). Therefore, whatever the motivation for Wagner's choice of the log-normal form for $g(\tau)$, it proves to have been a good one.

There is one caveat, however. The log-normal distribution is symmetric about its maximum and can only generate similarly symmetric ϵ'' functions. Experimentally, asymmetric ϵ'' curves are frequently observed. Indeed, these may well be the norm. There is also a good physical basis for such asymmetry which can arise from the anomalous time dispersion of hopping and tunneling processes that are common in amorphous materials. These give a long-tailed power law t^{-n} type of decay characteristic mentioned earlier rather than the exponential decay assumed by Wagner and most of his followers until recently. More modern discussions of the form of the dielectric response function may be found [19-23].

Proceeding with the conventional treatment after Wagner, the equations above for ϵ' and ϵ'' with $g(\tau)$ given by Eq. (22) are simply extensions of Eq. (14) to a specific distribution of conductive response times and still do not contain any details about the shapes of the conductive particles. These are contained in a shape factor K . Sillars [9] gives values of K for the simple Maxwell model

$$K = \frac{q\epsilon'_1}{(1+q)\epsilon'_2}, \quad (23)$$

$$\tau = \frac{q (\epsilon'_1 + \epsilon'_2) + \epsilon'_2}{(1 + q)/\rho_2}, \quad (24)$$

and

$$\epsilon'' = (1 + 2q) \frac{\epsilon'_1 \epsilon'_2}{q (\epsilon'_1 + \epsilon'_2) + \epsilon'_2}, \quad (25)$$

where now q is the ratio of thickness of the conducting layer to the total thickness of the media between the capacitor plates.

Sillars shows the dramatic change in the loss tangent $\tan \delta$ that takes place when the conducting material, instead of being disposed in the form of a plane layer, is distributed in the form of small spherical particles. Figure 3, adapted from Sillars, shows this effect. Van Beek [24] in a valuable review article gives an extensive compilation from various sources of shape factors for a variety of geometries: two layer and multilayered planar systems such as Maxwell treated, systems of dispersed spheres (after Wagner), dispersed spheroids (Sillars), dispersed ellipsoids, conducting spheres and ellipsoids dispersed in insulating dielectric media, dispersed cylinders and rods, dispersed lamellae, colloidal solutions, and porous dielectrics. All of these are given in modern rationalized MKS units.

In addition, Van Beek gives some calculated results ϵ' and ϵ'' for several of these geometries using practical ranges of values of parameters and properties of particles and surrounding media to illustrate how the MWS effect can give very large apparent permittivities and dielectric losses for certain ranges of these parameters and sizes and shapes of dispersed particles. The results are sometimes dramatic. For example, a simple two layer planar system of the type given by Maxwell, having a low conductivity layer of thickness 10^{-3} mm with a 5 mm thick semiconducting layer of the same basic relative permittivity $\epsilon' = 2$ but a conductivity 10^4 times greater, gives a low frequency static permittivity $\epsilon' = 4450$ and a peak loss $\epsilon''_{\text{peak}} = 2224$ for a maximum loss tangent of about 0.5. The loss peak occurs at a frequency of 0.27 MHz in this case which might occur in practice with a heavily oxidized metal plate between two electrodes or an electrolyte between oxidized electrodes.

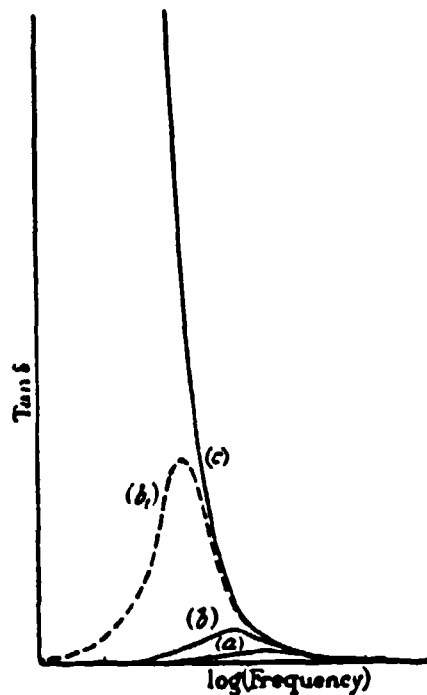


Fig. 3 - Loss angle of a given concentration of semiconducting material dispersed in an insulating dielectric as a function of the shape of the conducting material [9].

- (a) Sheet form normal to the applied field.
- (b) Spherical particles.
- (b') Spheroidal particles with major axes along the field.
- (c) Cylindrical particles extending from one face to the other of the dielectric.

Magnitude of MWS Effects

Of particular interest for the present study are the cases of conducting particles of various shapes embedded in insulating media with normal, relatively low permittivities and losses. For these cases formulas collected by Van Beek from several different authors do not agree with experiment. These formulas were derived for dielectric ellipsoids of various eccentricities and orientations with respect to the external applied field, and the transition to the case of high conductivity particles was made by letting the permittivity ϵ' of the ellipsoids become very large compared with that of the

surrounding medium. The resulting expressions for the overall permittivity of the inhomogeneous dielectric turn out to be fairly simple, but they do not predict the very large values of ϵ' and $\tan \delta$ that are found in, for example, neoprene with more than about 12% carbon black filler.

Polder and Van Santen [25] have proposed an expression for the resultant ϵ' that is proportional to the product of the concentration of conducting ellipsoids and their permittivities, so one can simply choose the latter to give as high a value as desired for the overall ϵ' , but this is not a very satisfying situation theoretically. Sillars' [9] treatment of the case of conducting spheroidal particles in a continuous matrix gives a more complex but also more detailed picture of the effects of the various parameters. But it, too, fails to account for the very large values of ϵ' observed experimentally. The Sillars results resemble those of Wagner shown in Eqs. (15)-(19) for spherical particles. Both Sillars' and Wagner's treatments emphasize the effects of conductive particles upon the positions and shapes of the dielectric functions ϵ' and ϵ'' , but the effects upon the absolute magnitudes of these functions are not adequately accounted for. A fully satisfactory treatment of the magnitudes of the dipole moment induced in a conductive particle embedded in a dielectric insulator involves the complex subject of screening in metals and semiconductors, as mentioned earlier. Though a completely satisfactory theory does not yet exist for this important subject, it is possible by relatively straightforward arguments to arrive at reasonable estimates of the magnitude of ϵ' and ϵ'' at very low frequencies sufficient to predict static permittivities that compare with observed values.

Consider a small embedded conductive particle of volume v and initially for convenience let the particle be a rectangular prism of sides ℓ and length ℓ' in the direction of an externally applied electric field E_0 . If there are n mobile charges (conduction electrons) per cm^3 in the particle, giving charge density ne where e is the magnitude of the electron charge, the total free charge in a particle will be $q = nev$. If the applied field E_0 were able to sweep all of the free charge to one end of the particle, the resulting dipole moment would be $p = \frac{1}{2}q\ell' = \frac{1}{2}env\ell'$, the factor $\frac{1}{2}$ arising as usual because on average the initially evenly distributed charge q moves half the length of the particle.

This simple analysis is incomplete, however, because it fails to take into account the fact that as the charge moves, it creates a counter field due to space charge accumulation at the downfield end of the particle at the interface with the insulating (or much lower conductivity) material surrounding the particle. Eventually the motion of the charges will stop when the counterfield balances the local applied field, and the space charge is then said to screen out the local field when the system is at equilibrium.

Most texts on solid state physics [26, 27] reproduce the standard treatment of the problem of screening in a conducting solid through the dielectric function $\epsilon(k, \omega)$.

This form of the permittivity is a function of both the circular frequency ω and spatial wavenumber k ($=2\pi/\lambda$) of an electromagnetic disturbance within the conductor.

The usual treatment is given in both the Thomas-Fermi and Lindhard approximations for the free electron gas in a metal or semimetal. The Thomas-Fermi expression is particularly simple in the static case when $\omega=0$:

$$\epsilon(k,0) = \epsilon_0 \left[\left[1 + \left(\frac{\lambda}{\ell_s} \right)^2 \right] \right] . \quad (26)$$

Here λ is the longest-wavelength electromagnetic wave that can "fit" the length of the sample in the field direction. In the example being considered, $\lambda=2\ell'$.

The quantity ℓ_s is the Thomas-Fermi screening length,

$$\ell_s = \left(\frac{6\pi n e^2}{E_f} \right)^{-1} . \quad (27)$$

where the Fermi energy E_f is given by

$$E_f = \frac{h^2(3n/8\pi)^{2/3}}{2m^*} . \quad (28)$$

In this expression h is Planck's constant and m^* is the effective electron mass. (Cgs units are used here: $e=4.8 \times 10^{-10}$ esu, E_f is in ergs, ℓ_s is in cm, $h=6.624 \times 10^{-27}$ erg-sec, n is cm^{-3} , and m^* is in grams.)

Equation (26) is consistent with the statement often made that the dielectric constant of a conductor (metal) approaches infinity. This is true in the Thomas-Fermi approximation only for an infinitely long conductor for which $\lambda \rightarrow \infty$. The more precise Lindhard expression for the dielectric constant of a metal, based upon a quantum mechanical calculation, leads to a small correction to the Thomas-Fermi form that is insignificant for particle sizes of the order of those of carbon fillers used in elastomers, namely a few hundred angstrom, though agglomerates of particles may be much larger.

The particle size in the field direction determines the magnitude of the permittivity through Eq. (26) which gives the dipole moment p per unit volume of the particle for a single particle through the classical relation $\epsilon = \epsilon_0 + p/E_l$, where E_l is the local field in the vicinity of the particle, and ϵ_0 is the permittivity of free space. Thus, $p = (\lambda/\ell_s)^2/\chi E_l$. If the applied field is E_a and the average permittivity of the composite sample is $\langle \epsilon \rangle$, then $E_l = E_a/\langle \epsilon \rangle$, provided the conducting particles are sufficiently widely dispersed not to disturb each other's local fields. When this is true, $p = (E_a/\langle \epsilon \rangle)(\lambda/\ell_s)^2$.

If the dipole-dipole interactions are ignored and the particles are regarded as independent and suspended in a medium, the electrical effect of the medium will be to reduce the applied field to

$E_t = E_a/\epsilon_s$, where ϵ_s is the relative static permittivity of the pure, unfilled medium rather than the average $\langle \epsilon \rangle$ of the composite medium plus particles. Since $\epsilon_s \ll \langle \epsilon \rangle$ in cases of interest here, the particle dipole moment per unit particle volume will be $p = E_a(\lambda/\ell)^2/\epsilon_s$.

Equation (26) gives the dielectric permittivity for a single, isolated particle without correction for the depolarization effect due to the shape of the particle. The depolarization factor F arises as a result of fitting boundary conditions at the surfaces of the particles. Depolarization factors are derived from classical theory and are given in any standard text on electromagnetic theory. In SI units they are simple quantities for simple shapes; e.g., $1/3$ for spheres, 1 for a thin slab, 0 for a long thin cylinder, etc. Kittel [26] gives a useful graph of F vs axial ratio for ellipsoids.

The dipole moment of a dielectric particle is related to the local field E_t through the dielectric susceptibility, $\chi = p/E_t$. For an ellipsoidal dielectric particle in a uniform local field, classical theory gives

$$p = \chi E_t / (1 + \chi F) . \quad (29)$$

Note the similarity of this expression to the equation for effective gain of a negative feedback amplifier (or any linear feedback system). In Eq. (29) χ plays the role of the open circuit gain of the amplifier, and F is the feedback factor, the fraction of output fed back to the amplifier input. This is a useful analogy since it gives in a more familiar form the way in which the net response depends upon F . When χF is small compared with unity, the net gain is large; i.e., and determined entirely by χ . When χF is large, on the other hand, the net gain is determined entirely by F independent of the gain of the amplifier itself.

The presence of space charge in conductive particles, in contrast to insulating particles to which the classical analysis applies, modifies Eq. (29) by changing F in ways not yet known nor easily calculated except for a few very simple geometries. The space charge values of F will, in general, be different from those calculated for dielectrics.

Within a conductive particle the depolarizing field $E_d = -Fp$ reduces the local field by the amount E_d , giving a lower value for the local field

$$E_t' = E_a[\epsilon_s(1 + \chi F)]^{-1} . \quad (30)$$

With $p = \chi E_t'$ and $\chi = (\lambda/\ell)^2$ one has from Eq. (26) and the classical definition $\epsilon = \epsilon_0 + \chi$ an expression identical to Eq. (29), but with the value of F different from the one in Eq. (29), determined for the space charge case. The corresponding equation for the permittivity can be written

$$\epsilon' = \epsilon_0 + \frac{\chi}{1 + \chi F} . \quad (31)$$

Two limiting cases of interest, $\chi F \ll 1$ and $\chi F \gg 1$, are the same as before. The first of

these gives $\epsilon' = \epsilon_0 + \chi/\epsilon_0$. This case will arise when the geometry of the particles gives $F=0$, regardless of the magnitude of χ . In this case, χ can be large if λ , which is approximately twice the length of the particle parallel to the local field, is large, i.e., for long particles oriented along the field direction.

For graphite, and presumably also for amorphous carbon which has nearly the same conductivity, Ashcroft and Mermin [27] give $n = 3 \times 10^{18} \text{ cm}^{-3}$ and the effective mass of the electron, $m^* = 0.06m_0$, where m_0 is the mass of the free electron. For these values the shielding length is approximately 15 \AA . Since colloidal carbon particles used as fillers in elastomers have minimum diameters of about 300 \AA by electron microscope measurement, the value of λ/ℓ_0 is at least 20, so ϵ' will be at least 400. This is in the general range of experimental values found for carbon black filled elastomers in this study at low frequencies.

The other limiting case, $F\chi \gg 1$, gives $\epsilon' = \epsilon_0 + p/\epsilon_0 F$. This case can only arise when $F > 0$, and for most particle shapes it is reasonable to expect that F will be well above zero. Therefore, ϵ' will not be very large for this case, but its value will depend directly upon the magnitude of F , independent of χ , as expected from the feedback analogy.

It is evident that values of F are important to determine which of the two cases is dominant for a given type of conducting particle. A full treatment, to include both screening and proper boundary conditions on the local and internal fields in the particles, appears to be a rather formidable task. Without carrying out such an analysis, a strictly correct formulation of Eq. (31) cannot be given, but two simple special cases can be treated. Electric field lines at a conductor surface increasingly approach normal incidence as the conductivity becomes large, and the depolarization factor approaches zero for cases in which most of the field lines are normal to the surface. This is the situation even in the presence of space charge for flat conducting slabs whose faces are perpendicular to the applied field, and in this case $F=0$ with or without space charge. At the other extreme, for long thin conducting needle-like particles, because the E-field is tangent to the particle surface on the sides and the tangential component of E is continuous across a boundary in general, even in the presence of space charge, it is reasonable to expect that in this case also $F=0$, as it is in the classical dielectric case for this needle-like geometry. The value of F for other shapes will, of course, differ in the presence of space charge from the pure dielectric values. In what follows, F will be taken to be zero.

There is reason to question the applicability of much of what has been said above whenever agglomerates rather than compact, dense carbon particles are responsible for MWS effects. In the frequency range covered in this work, it is generally the case that carbon agglomerates dominate low frequency effects. Estimation of F for dendritic particulates presents special problems not yet addressed. To deal first with concentration, let there be N conductive particles per unit volume in the composite material. The particle mass concentration c is then mN/ρ_0 grams of filler particles per gram of composite material. Here m is the mass of a particle, assumed to be the same for all

Let ρ' be the density of the material of the conductive particles and v be the mean particle volume, so the particle mass $m = \rho'v$. Then $c = \rho'vN/\rho_0$, and the effective static permittivity of the composite will be the simple mass-weighted sum of contributions from the pure matrix and from the conductive particles provided the concentration is small enough that interactions between particles may be neglected. Thus, ϵ' may be written for the non-interacting particle case

$$\epsilon' = (1-c)\epsilon_0 + c \left[\epsilon_0 + \frac{(\lambda/\ell)^2}{[\epsilon_0 + F(\lambda/\ell)^2]} \right] \quad (32)$$

In the carbon filled elastomers of interest in this study, c ranges from about 8% to 25%, λ/ℓ is ≥ 20 , and ϵ_0 is 3-6. Within this range of parameters one can account for values of ϵ' from about 10 up to about 45 for particles that are roughly cubic with $\ell' \approx 300 \text{ \AA}$. For more elongated particles ϵ' goes up approximately as the square of ℓ' , so ϵ' can easily increase to very high values. On the other hand, for particle agglomerates, and particularly for those loose enough in structure to have low conductivity mediated mainly by hopping and/or tunneling mechanism, the screening length is no longer given by the simple Fermi-Thomas theory, and the applicability of our screened field results is open to question. The simple approximate theory presented here is capable of giving magnitudes of the static dielectric constant that are in rough agreement with experiment for quite reasonable values of the relevant parameters but only for dense single particles.

Dynamics of Delayed Conduction Relaxation

Turning next to the dynamics of the formation and relaxation of dipoles that arise due to charge migration in conductive particles, it is important to consider the time response of the conduction process following the application of a local electric field. In amorphous conductors, and also in some semiconductors and semimetals with deep trapping centers, part of the conductive charge motion may be delayed, often by quite long times, due to trapping of free electrons at defects in the solid. The tunneling and hopping conduction mechanisms are inherently delayed. Therefore, it is useful to consider the conductivity as a complex quantity $\sigma^* = \sigma' + j\sigma''$. The real part σ' accounts for the conduction current in phase with the applied time-dependent field while the imaginary part σ'' accounts for current that lags the field by 90° . Note that in this case σ' is the lossy part while σ'' is the storage part of σ^* . Thus, σ' combines with ϵ'' to give the net loss in the composite material while σ'' and ϵ' together form the storage part of the total permittivity of the material.

The relevant Maxwell equation may now be written in the following form for an applied field oscillating at frequency ω ,

$$J_1 = \frac{\partial D}{\partial t} + J = (j\omega\epsilon'' + \sigma'')E = j\omega E \left[\left(\frac{\epsilon' + \sigma'}{\omega} \right) - j \left(\epsilon'' + \frac{\sigma''}{\omega} \right) \right], \quad (33)$$

where D is the dielectric displacement proportional to the storage part of the permittivity ϵ' plus the out-of-phase part of the conductivity σ'' . J is the current density in phase with the applied electric field, including both σ' and the dielectric loss permittivity ϵ'' . This leads to the identification of the real or storage part κ' of the overall complex permittivity κ^* with $(\epsilon' + \sigma'/\omega)$, and the overall loss permittivity κ'' with $(\epsilon'' + \sigma''/\omega)$, where $\kappa = \kappa' - j\kappa''$.

It is clear from the result

$$\begin{aligned} \kappa' &= \epsilon' + \sigma'/\omega, \\ \kappa'' &= \epsilon'' + \sigma''/\omega, \end{aligned} \quad (34)$$

that at sufficiently low frequencies, the $1/\omega$ factor in the conduction terms will make these terms dominate over the polarization processes, and σ' and σ'' will become the important parameters. The frequency at which conduction begins to dominate will, of course, increase as the conductivity itself rises, so as either the concentration of conducting particles in a composite elastomer or the conductivity of the individual particles increases, σ'' will rise and so will the crossover frequency at which the $1/\omega$ characteristic frequency dependence becomes important. The conductivity can also vary markedly at constant conductive particle concentration due to agglomeration and restructuring of the particles [16]. For this reason, there may not be a simple relation between concentration and the conductive contributions to κ^* .

It should also be emphasized that in Eq. (34) all four quantities on the right hand side are frequency dependent, giving rise to a wide range of possible frequency variations of κ' and κ'' . In general, however, the region of strong frequency dependence of ϵ'' does not overlap the region of strong dependence of σ' . This permits separation of the dipole and conduction effects in favorable cases, and in such cases it becomes possible to isolate and study the peculiarities of the delayed conduction embodied in σ'' , making these dielectric measurements on composites a potentially useful tool for investigating dispersive charge transport in such solids.

The crossover frequencies at which the dipolar and conductive contributions to κ' and κ'' become equal are best found from experimental data plotted as $\log \kappa$ vs $\log \omega$ or $\log f$. As ω decreases, these plots should approach straight lines with slopes -1 according to Eq. (34), provided neither σ' nor σ'' depends upon ω . At frequencies well above crossover, the frequencies are in most cases still well below the range where ϵ depends appreciably upon ω . In such cases, the frequency dependence of both κ' and κ'' will be rather flat. The crossover value ω_c can then be found at the intersection of the two asymptotic straight lines, one with slope -1 and the other with slope = 0 for the lossy part κ'' . In the transition region near ω_c , any structure that appears in κ' would ordinarily be attributable to $\sigma''(\omega)$, while structures in κ'' in this region would likely be due to σ' .

Experimentally, however, matters are not so simple. The low frequency limiting slopes of $\log \kappa'$ and κ'' vs $\log \omega$ become linear but not necessarily with slopes of -1, as expected from Eq. (34). The slope of the real part κ' approaches -1 at sufficiently low frequencies, but the absolute value of the slope of κ'' remains less than one. This is due to the frequency dependence of σ'' which goes to zero as $\omega \rightarrow 0$ because σ'' is inherently an ac term, vanishing at dc. If the frequency dependence of $\epsilon'(\omega)$ in this range were well enough known, $\sigma''(\omega)$ could be determined from the low frequency experimental data.

Dispersive Transport Effects

Non-integer slopes of the kind observed at low frequencies in carbon filled elastomers are found in responses of many other materials (see the reviews by Ngai [13], Rajagopal and Ngai [28], Rendell and Ngai [29], Jonscher [30], Scher, et al, [12]). Such nonlinear responses are believed by many workers to be universal, though there is some difference of opinion as to precisely what mathematical form the response function should follow. Two forms are presently in vogue, the stretched exponential and the non-integer power law. Both fall into the general category designated as dispersive transport. It will be shown presently that the power law is an asymptotic extension of the stretched exponential, so the two formulations are actually one and the same though they do not appear so at first glance, and this equivalence has generally been overlooked.

Jonscher [30] makes a particularly strong argument in favor of an asymptotic ω^β dependence of both real and imaginary parts of the dielectric susceptibility χ with β between zero and one for frequencies far below the loss peak, and an asymptotic $\omega^{\beta-1}$ dependence on the high frequency side. He provides evidence for the universality of this kind of frequency dependence for all types of dielectric response in a wide variety of materials, both conducting and non-conducting. In this respect, the power law behavior appears to apply to both the dipolar response and to the conduction response as well. It should be remembered that these are limiting behaviors of χ' and χ'' far from the loss peak or the χ' inflection point on plots of $\log \chi$ vs $\log \omega$. Behavior near the loss peak is not prescribed by the asymptotic response, of course. In attempts to bridge this gap, hybrid forms of the power law response have been proposed [30], such as $\chi'' [(\omega/\omega_0)^{\beta'} + (\omega/\omega_0)^{1-\beta}]^{-1}$ where β' and β are not necessarily equal, though they are both numbers between zero and one; ω_0 is the frequency of the loss peak χ'' or the inflection of χ' . One result of the power law response is that the ratio of loss to storage susceptibility $\chi''(\omega)/\chi'(\omega)$ reduces to the simple form $\text{ctn}(\beta\pi/2)$, independent of frequency, far from the loss peak region.

The high frequency behavior of carbon filled elastomers is dominated by dipolar processes that may be broadened and may be asymmetric but nevertheless have well defined loss peaks and inflection points in their storage permittivities. These features are not accounted for in any detail by the asymptotic forms emphasized by Jonscher. Ngai and coworkers, on the other hand, were able to fit the region around the loss peak and inflection point quite well with the stretched exponential

function in many different materials for both elastic and dielectric responses and for viscoelastic responses, as well.

Unfortunately, there is no closed form for the Laplace transform of the stretched exponential function $\exp(-t/\tau)^\beta$ except for the special values $\beta = 0.5$ and 1. Consequently, there is no general closed form for the frequency response, and it is not a simple matter to infer the frequency response characteristics from the current decay response in the time domain.

The low frequency asymptote can be found rather simply, however. Let $f(t)$ be the general response function in the time domain. Then it can be shown [31] that the frequency response $F(\omega) = \mathcal{L}_{j\omega} [-\partial f/\partial t]$, where $\mathcal{L}_{j\omega}$ is the Laplace transform for pure imaginary argument $j\omega$ (or the one-sided Fourier transform which is the same thing). For the stretched exponential, the time derivative $\partial f/\partial t$ may be expanded in a series in (t/τ_0) where τ_0 is one of the two parameters characterizing ϕ . This series may then be Laplace transformed, term by term, to give

$$F(\omega) = \beta \sum_{n=0}^{\infty} \frac{\Gamma[(n+1)\beta]}{n!} e^{-j\theta\pi/2} \omega^{-(n+1)\beta} \quad (35)$$

At high frequencies (low values of t/τ_0), the first term of the series is the dominant term, and $F(\omega) = \beta \Gamma(\beta) \omega^{-\beta}$. In this limit, the slope of the log-log plot is $-\beta$ in agreement with the power law model. At the other limit, low ω or $t \gg \tau_0$, the asymptotic form may be evaluated from the observation that Eq. (35) is a Laurent series expansion with an essential singularity at $\omega=0$. The asymptotic form is evaluated by the residue theorem as the limit as $\omega \rightarrow \infty$ of $j\omega F(\omega)$ [32], and the value is $\beta \Gamma(\beta) \omega^{1-\beta}$. This also agrees with the power law result at low frequencies, so the power law is seen to be simply the asymptotic form of the stretched exponential. Since the latter also appears to fit the experimental data near the loss peak well, the claims for universality of the stretched exponential also encompass those for the power law response. This would seem to resolve any controversies about the relative merits of these two models. They are in fact the same.

There still remains a problem of interpreting Jonscher's hybrid combination of low and high frequency power law expressions with different β 's which seem to work for some materials [30]. In fact, physical interpretation of the conventional stretched exponential response has not proven simple either, and various efforts have not yet led to a generally accepted physical picture of the underpinnings of this response.

The $\exp(-jn\beta\pi/2)$ term in Eq. (35), when expanded into $\cos(n\beta\pi/2) + j\sin(n\beta\pi/2)$, gives for the ratio of real to imaginary parts of the n^{th} term of the $F(\omega)$ expansion the value $\cot(n\beta\pi/2)$ which equals χ''/χ' . This agrees with the asymptotic value given by Jonscher for $\beta=1$. For frequencies nearer ω_0 , where the loss peak lies, more terms in the expansion must be included, and the simple $\chi''/\chi' = \cot(\beta\pi/2)$ relation no longer holds. The result is that the loss tangent near ω_0 , and in particular around the maximum value of $\tan \delta$, is no longer independent of frequency, as of course must be the case since $\tan \delta$ has a peak close to ω_0 .

It would be nice to be able to deduce the value of $\tan \delta_{\text{max}}$ analytically directly from Eq. (35), but this does not seem possible. Laplace transforms of the stretched exponential for many values of β have been numerically evaluated by Moynihan, Boesch, and Laberge [31] and more extensively by Moynihan [private communication]. From these calculated transforms, it is a straightforward matter to find the loss tangent for a given β . Values calculated from Moynihan's tables agree well with experimental results from this study for frequencies near ω_c .

However, one problem with Moynihan's approximate transform of the stretched exponential function is that his tabulated values give no peak in the loss tangent as a function of frequency within three decades of frequency below or four decades above the loss peak, the range of his tabulated values. On the other hand, the asymptotic $\omega^{-\beta}$ frequency dependence of the stretched exponential response does lead to a finite asymptotic $\tan \delta = \text{ctn}(\beta\pi/2)$ in the low frequency limit. Experimental data on some carbon filled neoprenes give a well defined $\tan \delta$ peak not far below the high frequency dipolar loss peak at ω_c , and the $\tan \delta$ is properly bell-shaped, showing every evidence of a monotonic decrease away from the peak in both directions. The reason for the failure of Moynihan's approximation to give a peak in $\tan \delta$ remains a puzzling feature that may be simply an artifact of the approximation when extended too far from the critical frequency ω_c . It appears likely, therefore, that the Moynihan evaluation of the Laplace transform is useful only in a restricted range of frequencies on either side of the loss peak.

Summary of Theoretical Status

The status of the theory of the MWS effect in particular, and dielectric response in inhomogeneous materials in general, may be summarized in the following way.

First, the dipolar response, largely due to rotational alignment of permanent dipoles in the polymer chains of the elastomer, generally occurs at relatively high frequencies, well above frequencies at which MWS conduction effects are important. Therefore, dipolar dielectric effects can usually be studied in relative isolation from MWS effects.

The simple, single response-time Debye model for dipole rotation is not adequate to account for the observed dielectric response at high frequencies, but it provides a convenient, if overly simple, initial model. A better representation of the real response appears to be given by the two-parameter, stretched exponential response function. One parameter, τ_c , locates the position of the loss peak, while the other, β , determines the width and asymmetry of the loss peak and its associated inflection region of the storage part of the complex permittivity. Both parameters are functions of composition and microstructure of the material, and they also depend upon temperature and pressure and possibly the past history of the sample.

There are exceptions to the rule that ordinary dipole and MWS effects are well separated in frequency. If conduction takes place in sufficiently small particles dispersed in the polymer, the particles mimic rotating dipoles in their frequency response. The time scale for the response is determined approximately by the transit time for a mobile charge to cross a particle, and this can be in the subpicosecond range for colloidal-size particles with relatively high conductivity. Carbon black particles are a good example; they may be only a few hundred angstrom in diameter, and their conductivity, while not in the range of a typical metal, is nevertheless large enough to place loss peaks at infrared frequencies.

At low to very low frequencies MWS effects are almost always present without any interference from dipolar influences. Again, their presence is revealed by large observed values of κ'' , but in this case there is a large trend upward as frequency decreases in both real and imaginary parts of κ^* . It is possible for these low frequency effects to occur without appreciable dc conductivity, but it is likely that this effect will be too small to be observable if it happens because of the very small conduction currents present in such cases. Usually, low frequency MWS effects occur as a result of agglomeration of conducting particles into larger, longer aggregates that are likely to form percolation paths for conduction through the sample. In the present work when carbon filler was present in concentrations above the percolation threshold, both dc conduction and the MWS effects increased markedly.

Low frequency MWS effects are complicated by the presence of both in-phase and quadrature components of conduction. The latter are conduction currents delayed by being trapped at impurities, interfaces, or structural defects particularly prevalent in amorphous materials, or the conduction electrons may be delayed having to hop or tunnel through barriers due again to structural defects of amorphous origin. Such slow or dispersive transport can introduce a large out-of-phase component into what is normally regarded as simple conduction, and this component is both dispersive and frequency dependent.

Though the various low frequency effects combine in complex ways to give the observed overall response, empirically these responses appear to fit the same, relatively simple two-parameter stretched exponential model as the simpler rotating dipoles. This fact is both a blessing and a curse for interpretation of results. The blessing is that there are, after all, only two parameters to contend with. The curse is that, as in the case of statistical thermodynamics, averages over large numbers of microsystems yield macro observables with few variables but at the same time effectively obscure the underlying processes at the microscopic level. One is prevented from working backward from macro to micro scales and is forced to devise micro models, perform the averaging which is not trivial in most cases, and then compare the results with experiment. The problem is that there may be many models that give similar macroscopic results. This is the major reason why it has been so difficult to give a good physical interpretation of τ_0 and β .

EXPERIMENT

Two types of dielectric measurements constitute the experimental techniques employed in the present work. One, the bridge method, is commonly used and operates in the frequency domain over a frequency range from low audio (≈ 20 Hz at the low end) well up into the megahertz range (to a high limit of ≈ 20 MHz in this work). The other method operates in the time domain and is useful at frequencies from millihertz, or lower, up to about one kHz, providing a sizable region of overlap with the bridge measurements. The time domain method is a modification of what has usually been called the pulsed or dc transient method because it commonly makes use of an input step function voltage applied to a dielectric sample in a parallel plate type holder in the form of a parallel plate capacitor. Charging or discharging currents are measured as functions of time following a step-type change in capacitor voltage. A one-sided Fourier transform (or a Laplace transform with pure imaginary argument) of the time derivative of the time-varying transient current can be shown to give both real and imaginary parts of the complex dielectric permittivity ϵ^* [1, 6, 31].

The samples were in the form of 2-in. diameter circles cut from flat sheets. Sample thicknesses ranging from ~ 0.2 in. to 0.85 in. were measured. Samples were prepared by standard procedures from formulations that are commonly used for NRL-USRD underwater applications [33, 34, 35]. Measurements were usually made on samples with silvered faces. The silver was applied by spraying an air-drying silver paint thinned with amyl acetate from a small CO₂ powered airbrush. The paint thickness was sufficient to give a good smooth conductive coating, and edges were masked to prevent shorting or current leakage around the edges. A few samples were measured with brushed silver air-drying paint and some were measured without any conductive surface coating. The airbrushed surfaces gave by far the most reproducible results.

Samples were held for measurement in a General Radio Type 1690 Dielectric Sample Holder that maintains a constant, light pressure upon the sample faces by spring force. This pressure is maintained when the holder is heated or cooled, and the plates of the holder are moved by a micrometer mechanism so the plate spacing can be monitored accurately and corrections made for creep of the sample if necessary.

The sample in its holder was placed for measurement in an insulated, heated and cooled box. An external Endocal heating/cooling bath provided a flow of coolant at constant temperature to copper coils inside the box, and the box temperature was measured with a laboratory mercury thermometer inserted through the top. The whole apparatus was kept in an airconditioned lab, and the sample temperature could be held constant to ± 0.1 °C. Whenever the temperature was changed, at least 6-8 hours were allowed to elapse before any measurements were made to be sure the sample had come to equilibrium. Equilibrium in this case does not merely mean constant temperature, which is established much sooner, but the sample must relax elastically and dielectrically which is a much

slower process especially at low temperatures. With this setup measurements could be made from about -15°C to $+40^{\circ}\text{C}$ which was as high as desired to avoid thermal deterioration of any of the samples.

The bridge measurements were made on two General Radio Capacitance bridges. A Type 716-C was used for low frequencies from 20 to 100 kHz. Frequencies above 100 kHz were measured on a GR Type 716-CSI which is similar to the 716-C but designed for higher frequencies. Bridge nulls were detected with an HP 400D vacuum tube voltmeter (VTVM) capable of nulling the bridges to within a few microvolts. The sensitivity of this detector falls off above about a megahertz, so for higher frequencies a shortwave radio receiver was substituted for the VTVM. The input voltage to the bridge was kept small, under 0.5 v, to avoid nonlinear effects that began to appear at driving voltages above about 1 v. In the frequency range above about 200 kHz, the coaxial connecting cable between sample holder and bridge behaved increasingly like a short waveguide, and it was necessary to correct for cable impedance variation with frequency.

When measuring samples that exhibited appreciable MWS effect, frequently either the capacitance or the dissipation or both exceeded the range of the bridge, and it was the practice in these cases to place a small 473 pF mica capacitor in series with the sample holder at the holder terminals. Corrections were then made for both the capacitance and the very small losses of the added series capacitor. With this modification, the highest capacitances and losses encountered in our samples could be brought within ranges of the bridges.

Bridge measurements were made manually and transferred to a spreadsheet; the data were reduced, smoothed, and graphed by computer.

Initially, the pulse decay technique was used in a straightforward way. A small dc voltage, again small to avoid nonlinear effects, was switched on by a solid state switch to the sample in the same GR holder used in the bridge measurements. A very low input impedance operational amplifier in series with the sample acted as a current-to-voltage converter or current amplifier. This amplified the charging current giving an output voltage waveform that could be digitized and stored in a Nicolet "Explorer" digital storage scope. The current amplifier was a Keithley Model 428 with a fast response suitable for such applications. The resulting waveforms superficially resembled simple exponential decay curves, but they actually contained a continuous distribution of time constants.

Data reduction in this case was also done by computer. Three methods were used at various times. The simplest method was devised by Hamon [36]. It is valid for currents with an algebraic type decay of the form t^{β} with $0.3 < \beta < 2$, and it gives ϵ'' directly, but not ϵ' . The value of ϵ'' at frequency f is proportional to the current at time $t = f/10$ from the onset of the voltage divided by f . The Hamon reduction seems to give good results down to frequencies a little below the frequency at which ϵ'' has its peak, but the accuracy deteriorates rapidly below that point.

A second reduction method is described by Moynihan, Boesch, and Laberge [31]. It is based upon an approximation of the current decay function as a weighted sum of simple exponential decays. The weighting function in this case is the (unknown) distribution function for the time constants. The case for a continuous distribution is a simple extension of the discrete case. Moynihan et al. showed that the dielectric modulus $M^* = 1/\epsilon^*$ can be expressed in the simple form of a purely imaginary Laplace or one-sided Fourier transform of the time derivative of the current decay curve. This is amenable to computer calculation and is the favored method for current decay data.

Moynihan also tabulated the frequency dependence of the real and imaginary parts of the dielectric modulus M^* for a stretched exponential form of decay curve $I = I_0 \exp[-(t/\tau)^\beta]$ that was mentioned earlier as being a prevalent time response for many materials and different types of processes. This function has no closed form of Laplace transform except for the special values $\beta=0.5$ and 1. Moynihan's tabulated values are convenient for finding the values of the parameters β and τ_0 .

Two experimental difficulties made the pulse decay method, as outlined above, less attractive than it first seemed and led to a modification that will be described below. The first problem with the decay method is degraded accuracy at the high-frequency end of the spectrum. The origin of this difficulty was the limitation on the sampling rate of the digital scope which in turn limited the highest frequencies that could be measured (by Nyquist's criterion). In addition, there was a limit to the frequency response of the current amplifier that imposed an additional high-frequency limit for small signals. It was possible to push these limits up into the tens of kHz range at some sacrifice in accuracy, so the pulse technique was not used above 1 kHz.

At the low end of the spectrum, a different limitation arose. The low-frequency information in the decaying pulse is to be found in the current at relatively long times after the voltage pulse is applied, but at long times the current has decayed to very low values, making accurate measurement increasingly difficult. To make matters worse, it is the time derivative of the current that is used to transform into the frequency domain, and at long times the slope of the $I(t)$ curve is nearly zero. Under such conditions amplifier noise and stray pickup, small as they were, were sufficient to seriously degrade the accuracy and, in the case of pickup, to introduce spurious peaks in the frequency spectrum.

To get around both of these limitations, the pulsed source was replaced by a low-frequency sine wave oscillator (Rockland 5100 Programmable Frequency Synthesizer), and the digital scope was synchronized precisely with the Rockland so the phase shift of the sample current with respect to the input voltage could be preserved in the digitized waveform. Since the input voltage and the resulting current were both measured, the method was actually a direct measurement of the complex impedance of the sample plus its holder and associated cabling. It proved possible with care to measure the phase to -0.2% over the entire frequency range covered in this manner (10^3 Hz to 1 kHz). With

both amplitude and phase of the current measured directly in this way, it was no longer necessary to go through the process of differentiation and Fourier transformation to reduce the data, which was already in the frequency domain. This also improved final accuracy.

An overlap of nearly two decades in frequency (20-1000 Hz) was maintained between the low frequency measurements and the bridge measurements. In this overlap range the low frequency values of ϵ' and ϵ'' were brought into agreement with bridge values so it was not necessary to calibrate the current gain of the amplifier accurately. The bridge measurements provided a convenient calibration datum in the overlap region.

The frequency range over which this technique can be used is very wide. It can be extended into the radiofrequency (RF) range at one end and into the millihertz range at the other. There is a commercial instrument, the GenRad Digibridge that, contrary to its name, is not really a bridge but an impedance measuring instrument that uses the same basic technique as described above over the range ~ 20 - 70 kHz. In this instrument, however, phase is measured by the time delay between two zero crossings of the waveform, a more conventional method than the use of a digital scope for precise phase measurement.

It would have been advantageous to employ a very-low-frequency lock-in amplifier to improve signal-to-noise ratio had such an instrument been available; at higher frequencies lock-ins are readily available. An alternative method of noise reduction would be to use a summing digital storage scope such as the Tracor-Northern NS560 Signal Averaging Computer, or a low frequency boxcar averager, which digitizes repetitive waveforms on each cycle and adds the amplitudes at each point of the waveform. In this way, several hundred such waveforms could be superimposed with the result that the random noise would tend to cancel or average toward zero while the signal would add.

In the present work, such instruments were not on hand so noise reduction was performed by smoothing the final calculated values of ϵ' and ϵ'' as functions of frequency. A simple, unweighted, 9-point moving average method, performed by spreadsheet calculation, proved convenient and satisfactory. Some distortion at the ends of a data set is introduced by this method, but such distortion is troublesome only if the data vary rapidly at the ends which was not the case here.

RESULTS AND DISCUSSION

Neoprene formulation 5109G has no carbon filler added, so it provides a baseline against which to compare the effects of added carbon. Samples, all prepared in the same way, but with added carbon black filler, are designated 5109K (8% C), 5109L (12.8% C), 5109S (21% C), 5109S/2 (23% C), and 5109 (26% C). The room temperature resistivities of these samples as measured in this work are shown in Fig. 2. The percolation threshold for conduction through the sample thickness (≈ 2 mm) is approximately 16% carbon black in this particular series of samples.

Figures 4-8 show the measured dielectric permittivities ϵ' and losses ϵ'' as functions of frequency on a log scale for a temperature of 300 K. Figure 4 is shown for 5109G with no carbon black. Its low frequency relative permittivity is 7.0 at 100 Hz, and its loss tangent is a low 0.014 at this frequency.

These are reasonable values for unfilled neoprenes (poly 2-chloro-1,3-butadiene) which contain chlorine and, therefore, have relatively large permanent dipole moments. The relatively small loss peak at 4 MHz ($\tan \delta \approx 0.12$) would appear to be a simple dipole rotation peak were it not for the fact that this peak increases markedly as the carbon black content rises, particularly when it is above the percolation threshold value.

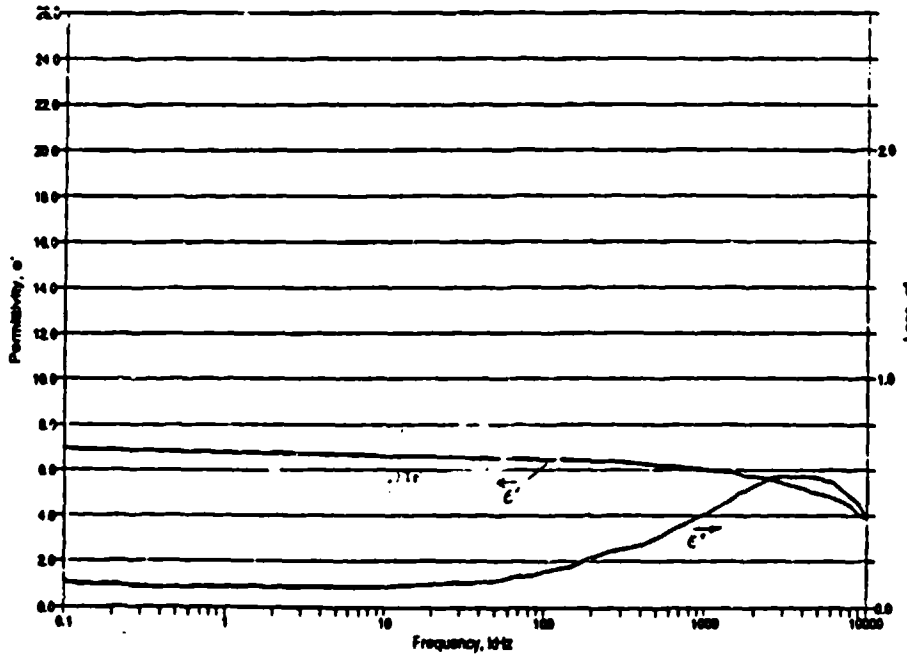


Fig. 4 - Relative permittivity ϵ' and loss ϵ'' for 5109G Neoprene at 27°C. Carbon content of 5109G is zero.

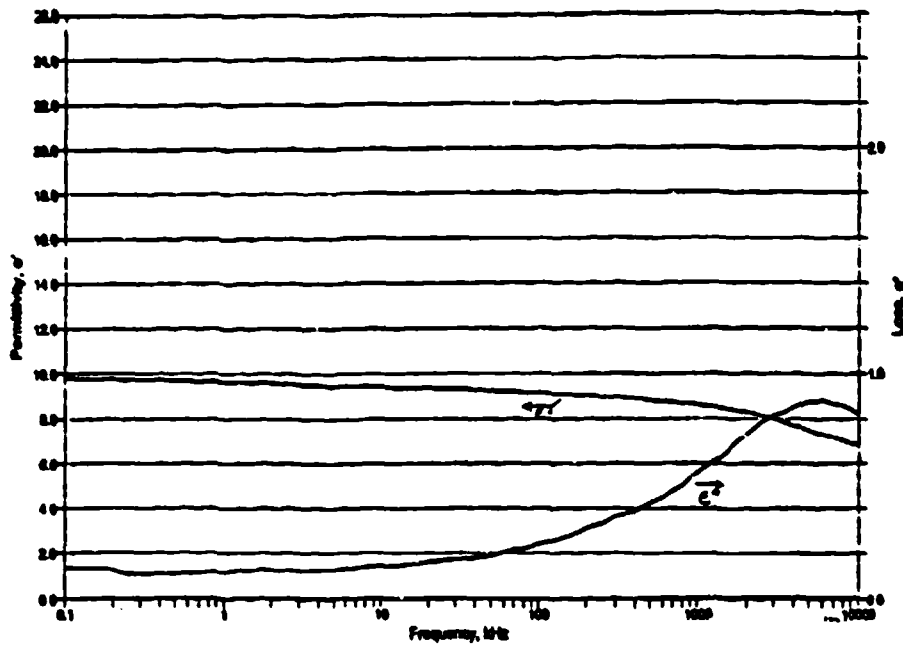


Fig. 5 - Relative permittivity ϵ' and loss ϵ'' for 5109K Neoprene at 27°C. Carbon content is 8% by weight.

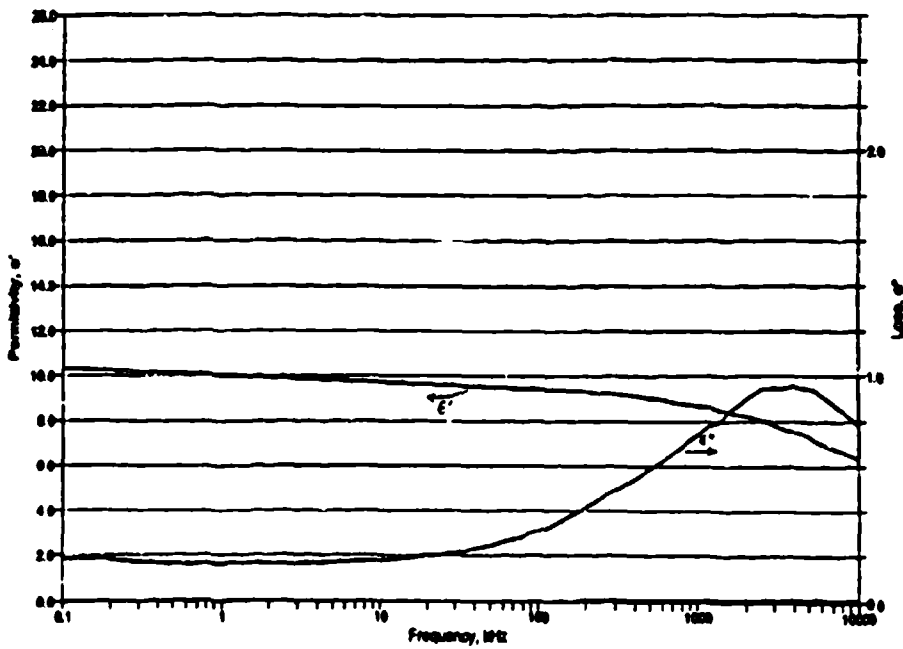


Fig. 6 - Relative permittivity ϵ' and loss ϵ'' for 5109L Neoprene at 27°C. Carbon content is 12.8% by weight.

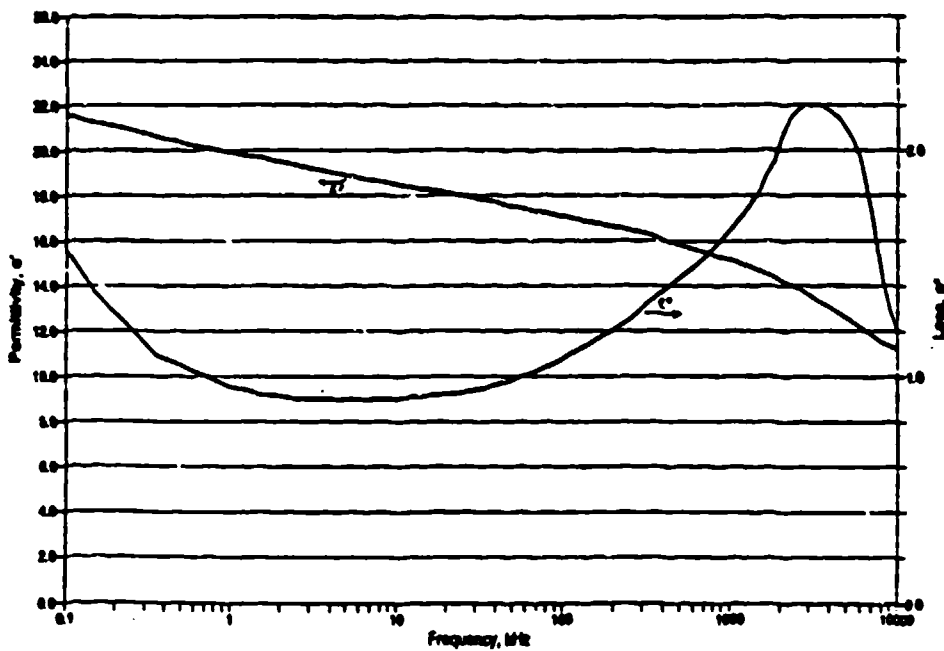


Fig. 7 - Relative permittivity ϵ' and loss ϵ'' for 5109S Neoprene at 27°C. Carbon content is 21% by weight.

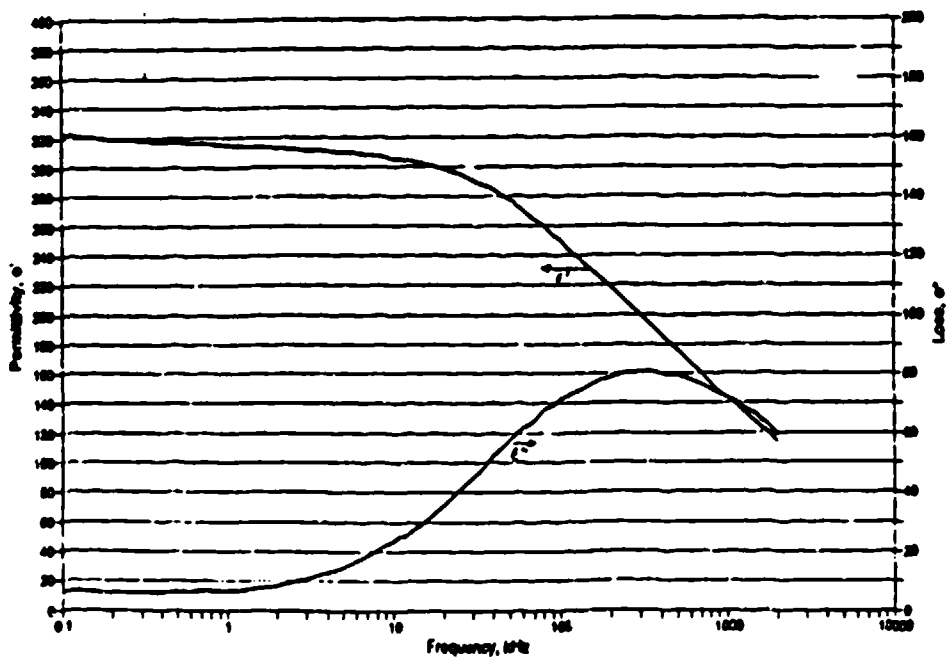


Fig. 8 - Relative permittivity ϵ' and loss ϵ'' for 5109 Neoprene at 27°C. Carbon content is 26% by weight.

Figure 9 is a plot height of this loss peak against carbon content for the neoprene series 5091G through 5109. The loss curves from which these data were taken are found in Figures 4-8. The magnitudes of the peaks are approximately proportional to carbon content up to the percolation threshold where ϵ''_{max} then rises exponentially at a high rate.

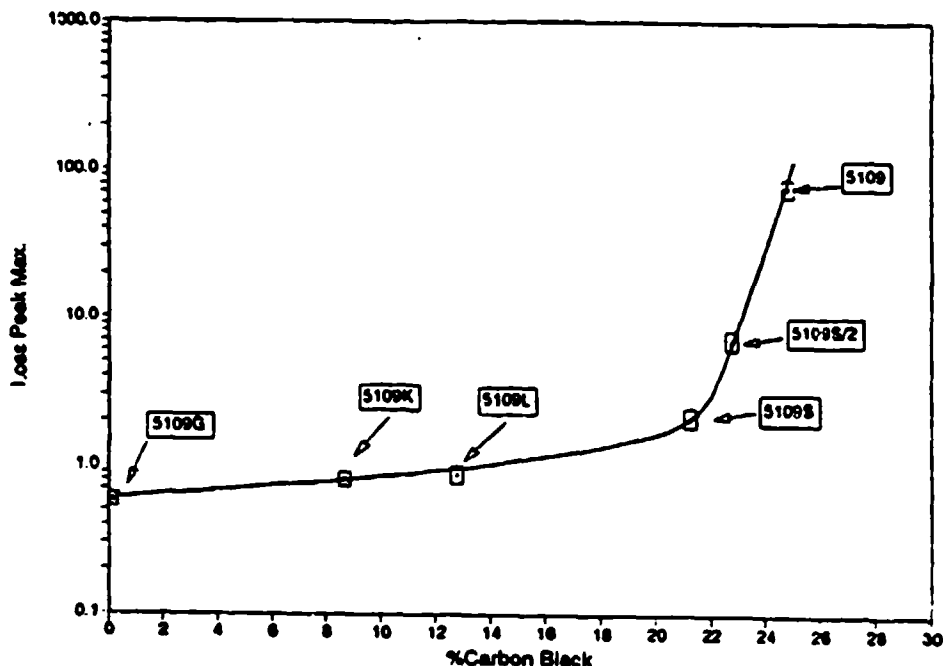


Fig. 9 - Loss peak magnitude ϵ''_{max} as a function of carbon black content for 5109 series of neoprenes.

The samples 5109S4 and 5109S3, with 8% and 12.8% carbon black respectively, both well below the conduction threshold, show only a small dependence of ϵ' and ϵ'' on carbon concentration. It is evident that a little below the 20% carbon content of 5109S a substantial internal change takes place that affects the dielectric properties as well as the conductivity (Fig. 2). The similarity between Figs. 2 and 9 suggests that clustering of carbon black particles in the material is responsible for the large increase in permittivity at the percolation threshold. It seems likely that the same mechanism that gives rise to percolative conduction paths through the full sample thickness also gives rise to very large dipole moments and losses via the MWS effect.

Clusters of carbon particles can form at all carbon concentrations, but the number and sizes of the clusters increase rapidly with concentration up to the percolation threshold [37-38]. These clusters, even when they are below the threshold, still form sizable conductive paths within the material in which large dipole moments can form by movement of conduction electrons under the

influence of an applied field. Thus, under ac excitation sizable MWS effects can be present below the percolation threshold, and these can give loss peaks at high frequencies provided the carbon clusters are small and reasonably conductive.

The morphology of these clusters is not well defined. However, they probably form dendrites [37]. If the carbon particles that make up a cluster are in good conductive contact, meaning that there is no significant potential barrier to electron transport across the interface between them, then they form a single large carbon particle as far as conduction is concerned, and the relevant time constant, $\tau = \rho\epsilon'$, discussed in an earlier section, still determines the frequency where the loss peak occurs (in the infrared as pointed out earlier). However, if there are interfacial potential barriers between carbon particles that make up a cluster, then conduction across the barrier between individual carbon particles in a cluster will be considerably retarded, and the applicable time constant for the process will be much longer. Conduction across such barriers will take place by a mixture of tunneling and thermally activated hopping mechanisms. The number of such barriers that slow the development of a conduction dipole in time will increase rapidly with cluster size. Therefore, the simple time constant τ of Maxwell and Wagner which involves only the properties of the pure carbon itself would no longer determine the overall response time of the conduction dipoles. Instead, the response time would be dominated by slow electron transport across the interfaces between carbon particles in a cluster and would also be a function of cluster size.

Another likely possibility is for the individual carbon particles to be attached chemically to polymer molecules. A clean carbon surface is chemically active because of the unsaturated p-electron orbitals at the surface. These "dangling bonds" readily chemisorb other materials with free bonding electrons. Of course, the carbon surface is anything but clean initially, but when the carbon black is mixed with other ingredients and raised to high processing temperatures, bonding with the polymer is possible and is usually assumed to take place. If this is correct, then the picture is one of individual carbon grains, roughly 300-400 Å in diameter, bound up in a net of polymer molecules and rarely in good conductive contact with other carbon particles. Conduction can take place between two of these particles when, still cloaked in their polymer nets, they approach closely enough under thermal agitation. Since electron transport across a contact barrier between carbon particles depends exponentially upon the barrier height and temperature (in the case of hopping) or barrier width (in the case of tunneling), it follows that the conduction process can be many orders of magnitude slower than ordinary ohmic conduction. Moreover, the screening effects that were important for conduction within a single particle and which led to earlier estimates of the magnitude of ϵ' are no longer relevant for clusters where barrier effects predominate.

Lacking detailed knowledge about these carbon-carbon contacts for the present case, only a qualitative phenomenological picture can be given like the one above. Within this picture, it is entirely possible to have loss peaks in the 4 MHz range and below, as observed. In fact, if a quantitative relation between cluster size and charge transport response time in clusters were available, the position of this loss peak could be used to find the cluster size or size distribution

function, making the MWS effect a valuable analytical tool. Furthermore, such a tool could follow cluster development as a function of carbon concentration, processing conditions, etc.

In the 5109 neoprene elastomer series used in this work, experiment shows (Fig. 4) that a fundamental loss peak is present at about 4 MHz in 5109G which has no added carbon black filler. This observation clearly identifies this peak as not being due to carbon effects and as being most likely due to rotational orientation of the permanent dipoles of the unfilled polymer material itself.

It is a noteworthy feature of the curves in Figs. 4-8 that addition of carbon serves only to increase the magnitude of the 4 MHz loss peak without appreciably shifting its frequency or changing its shape. This is taken to mean that this peak, while due to permanent dipole rotation, is somehow enhanced by indirect action of the conduction dipoles induced in the carbon particles or clusters. Clearly, in 5109G the 4 MHz peak can have nothing to do with carbon since none was present in that sample. However, there is a strong enhancement of this loss peak when carbon is added, and the effect is particularly striking when the percolation threshold associated with conduction through the full thickness of the sample is passed, as Fig. 9 shows.

At any given frequency ϵ' (or κ') is the sum of all polarization effects that occur at higher frequencies. Therefore, the effect of adding carbon particles that do not agglomerate or cluster is present at all frequencies in the range of our measurements, so the measured values of ϵ' will increase uniformly in proportion to the carbon content over the entire frequency range of our measurements. There is an additional increase in ϵ' on passing through the 4 MHz loss peak that is proportional to the height of the loss peak ϵ''_{max} , as theory requires.

A possible explanation for enhancement of the 4 MHz loss peak by carbon black particles is offered along the following lines: When an external field is applied, a given carbon particle conductively polarizes almost instantaneously, following the local field with virtually no time lag. A large dipole is thus immediately induced in this carbon particle, and it gives rise to a strong local orienting torque that acts upon permanent polymer dipoles in the vicinity of the carbon particle. The presence of the carbon particle also mechanically strains the polymer structure locally, increasing the free volume there, thus facilitating rotation of the polymer dipoles in that region. This mechanism would act to enhance polarization of the polymer around a carbon particle. The result would be an increase in both ϵ' and ϵ'' at frequencies near the natural dipole orientation frequency of the polymer medium, i.e., in the vicinity of the loss peak of the unfilled polymer which is the 4 MHz peak in the present case. This enhancement at low carbon concentrations would be proportional to the amount of carbon present, as observed experimentally.

At somewhat higher carbon concentrations where clustering begins to be important, there are two different possibilities depending upon whether or not the carbon particles in a cluster form high or low conductivity interfaces. If the clusters have high conductivity, they may be treated simply as large carbon particles, meaning that they would still respond practically instantaneously to the applied

field, and the enhancement of the 4 MHz loss peak would mirror the development of cluster sizes and numbers with no shift to lower frequencies.

On the other hand, if the clusters exhibit low conductivity, as they certainly do when they extend through the sample thickness where they can be measured as the overall sample conductivity, then the clusters do not respond so rapidly to the applied local field. There are still conduction dipoles induced in the individual particles in each cluster, but in addition much larger cluster dipoles develop slowly as conduction proceeds through the cluster, a process that becomes slower the larger the cluster. As long as cluster dipoles form in times shorter than the polymer dipole rotation time, enhancement of the 4 MHz loss peak will be essentially the same as outlined above for the case of separated individual carbon particles. As clusters grow, the cluster dipole induction time will increase due to the slow conduction in clusters, and there will be an appreciable time delay before a cluster dipole can contribute any enhancement to rotation of the polymer dipoles. The result is that the clusters themselves no longer contribute much to the enhancement of the 4 MHz loss peak but instead give rise to their own broad loss peak at lower frequencies. However, individual carbon particles that make up the clusters will still continue to respond rapidly as though they were isolated and will still act to enhance the 4 MHz peak.

In other words, as the carbon clusters grow their polarization increasingly lags the field, i.e., the cluster loss peak shifts to lower frequencies. The 4 MHz peak of the polymer dipoles remains at the same frequency but is less and less subject to enhancement at that frequency by the shifted conduction dipole moments of the carbon clusters, though the enhancement effect of the individual carbon particles upon the 4 MHz polymer peak remains whether the particles are in clusters or not.

After the percolation threshold is reached, the maximum possible cluster size has also been reached, i.e., it equals the sample thickness. Beyond this point, there should be little or no further frequency shift in the contributions of the maximum size clusters which would then be shifted to the limiting very-low-frequencies characteristic of electrode effects. Since this maximum cluster length is directly related to sample thickness, it follows that the low frequency limit will depend upon the sample. It has been found experimentally, both in this work and elsewhere [12], that the very low frequency dielectric properties are indeed dependent upon sample thickness. Once past the percolation threshold, the sample conductivity will continue to increase due to formation of additional parallel conduction paths through the sample, and the very low frequency MWS contribution to κ'' will continue to grow in magnitude with addition of more carbon.

All of these effects may be seen in Figs 4-8. In Fig. 8, the 5109 sample with 25% carbon is well past the percolation threshold, and a shift of the high frequency ϵ'' loss peak to lower frequencies is evident. The 4 MHz peak has become submerged in the high side of the much stronger, broad cluster peak and is no longer resolved.

At the other end of the frequency range, conduction through the full thickness of the sample produces a marked rise in both κ' and κ'' as shown for 5109 in Fig. 10. (Note that at low frequencies where the conduction effects are significant the notation of Eq. (34) will be used, i.e., κ' and κ'' signify the net effective storage and loss permittivities instead of ϵ' and ϵ'' .)

In Fig. 10, both axes are on logarithmic scales, and a $1/f$ line is included to show how far down in frequency it is necessary to go to obtain ohmic conduction in this material. Over most of the frequency range shown in the figure, the loss appears to be dominated by dispersive transport [12], a mixture of tunneling and hopping conduction with the "long-tailed", power-law response characteristic discussed earlier. In thinner or more conductive samples, the $1/f$ characteristic extends to somewhat higher frequencies.

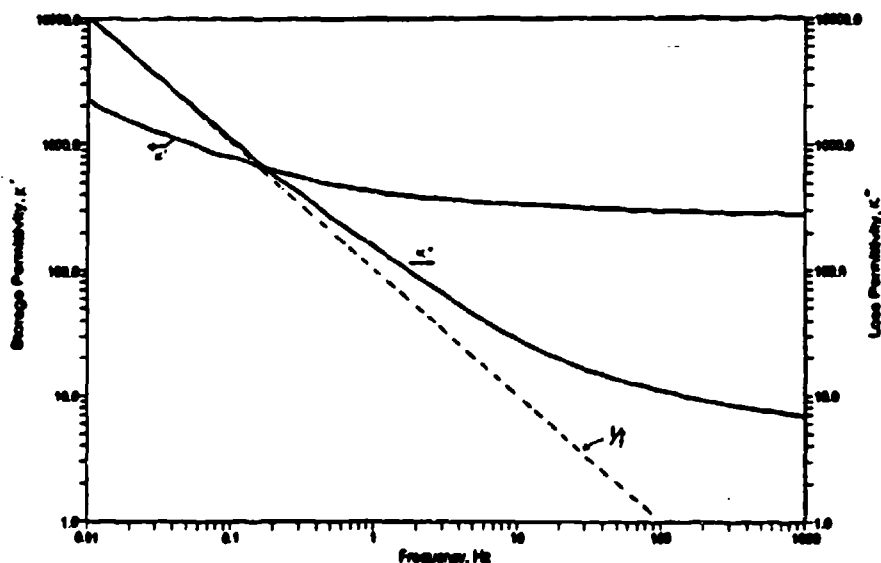


Fig. 10 - Relative effective permittivity κ' and loss κ'' at very low frequencies for 5109 Neoprene with 26% carbon at 27°C.

The curves in Fig. 10 are the real and imaginary parts of the total response, κ^* . The real part, $\kappa' = \epsilon' + \sigma''/\omega$, contains a $1/f$ component multiplied by the delayed conductivity σ'' while the imaginary part, $\kappa'' = \epsilon'' + \sigma'/\omega$, has a contribution from the ordinary ohmic in-phase conductivity σ' . The latter is not considered to have any significant temperature dependence, but σ'' , depends strongly upon temperature by virtue of its connection with hopping and tunneling mechanisms. Since it represents "slow conduction", it is an inductive term in contrast to the capacitive ϵ' term. It is inductive because the conduction current it represents lags the applied field rather than leads it as does the displacement current represented by ϵ' .

The $1/\omega$ factors in both κ' and κ'' would lead to divergences as $\omega \rightarrow 0$ unless both parts of σ^* vanish at least linearly with frequency at very low frequencies. The practical distinction between in-phase conduction σ' and slow conduction σ'' becomes blurred at sufficiently low frequencies. The

fact that there exists a finite dc conductivity means that σ'' must eventually become proportional to ω at sufficiently low frequencies, making both σ'/ω and σ''/ω constant as frequency goes to zero.

At high frequencies σ'' must vanish since it is a slow conduction term by definition. At zero frequency σ'' must also vanish because it is defined only for ac currents. Thus, $\sigma''(\omega)$ must have a peak of some sort at intermediate frequencies. This peak may be, and probably is, quite broad and indistinct because hopping and tunneling time scales are poorly defined. The σ'' peak may also lie almost anywhere below the polymer dipole rotation peak frequency, but it will most likely be at relatively low frequencies, especially in heavily carbon filled elastomers containing a predominance of large clusters in which conduction will be relatively slow.

The study of dispersive transport that seems to be a feature of the σ'' part of κ' is a topic of much current interest in condensed matter physics, and it would be a matter of some basic importance to be able to extract this $\sigma''(\omega, T)$ feature cleanly out of the data. At present, this is still not quite possible. The place to look for the clearest view of σ'' seems to be in the transition region of the spectrum between the broad range where κ' is nearly constant and the onset of a strong $1/f$ trend. This region merits special attention using a series of four or five neoprenes having finer gradations of carbon content than present samples in the region 14% to about 18% carbon. This is primarily where formation of carbon clusters takes place and where there is the most rapid variation in both numbers and sizes of these clusters.

The particular choice of the 5109 neoprenes for the present work has no special significance. It was a matter of convenience because the materials to make up this series were on hand. Other filled elastomers are expected also to exhibit similar properties, and some of them may have properties better suited to such studies than the 5109 neoprenes. Also, only one kind of carbon black filler was used and only one processing procedure. There are many carbon blacks available with different basic particle sizes and clustering properties, and it has been shown that variations in processing have strong influences upon carbon black aggregation in 5109 neoprenes [33]. It would be instructive to obtain data on some of these other blacks and other modes of preparation.

Finally, the temperature dependence of the dielectric properties has not been extensively examined. Only a few low temperature measurements were made to assess the general features of temperature dependence. A more detailed study should cast some light on relative importance of hopping vs tunneling conduction since these mechanisms have different temperature dependences.

CONCLUSIONS

The material treated in this report covers a rather wide range of topics in several related areas of physics of amorphous and inhomogeneous materials, and it seems appropriate to attempt to summarize the more important aspects of the study, particularly as related to the original objectives of the work.

The original goal centered upon the prospect of being able to derive some information about the size and shape distributions of inhomogeneities, specifically of carbon black fillers in elastomers, through interpretation of details of the dynamic dielectric properties as measured by more or less standard methods requiring no elaborate equipment or special skills. The earlier work on the MWS effect in several types of materials with conductive particles added supported the expectation that this goal could be achieved in carbon filled elastomers, as well [16].

It has become clear in the course of this study that the dielectric response of carbon filled elastomers is a much richer and more complex subject than prior treatments of the MWS effect would suggest. The subject of the present work touches upon several areas at or near the forefront of contemporary condensed matter research such as the dielectric response of semimetals like carbon, mixed tunneling and hopping conduction and dispersive charge transport in amorphous materials, local vs mean field theory in such materials, free volume effects in dispersive transport and the secondary effects of local strain-induced free volume, interface effects between conductive inclusions and the polymer surroundings, clustering and agglomeration of the particles, and conduction in such clusters, to name a few. None of these areas have been considered in earlier treatments of the MWS effect, so the present investigation has served to reveal some of the subtleties of the problem that were unforeseen at the outset.

Despite the difficulties in making physical sense of the experimental results in light of the inherent complexities of the problem, some progress was possible through simplifications resulting from the fact that major features of the problem are, under proper conditions, positioned in different regions of the frequency spectrum where they can be studied in some degree of isolation. Even so, the real goal of using dielectric spectroscopy to reveal size and structure of carbon clusters within an elastomer has proved elusive mainly because of our ignorance about electronic conduction in such clusters. There are still too many undetermined variables in such conduction processes. Arbitrary adjustment of these variables can produce nearly any desired result, so one cannot work backwards from the experiment to identify a unique set of such variables, specifically cluster size and shape distribution, as one would require of a valid spectroscopy.

Though it has not proved possible to deduce finer details about the distribution of carbon in elastomers, it has been possible to obtain some useful qualitative information. For example, the results of agglomeration of carbon and the growth of clusters to form conduction paths through the material can be followed qualitatively from the experimental data on series of elastomers with varying

amounts of carbon. This has been done systematically in this study in only one type of elastomer, a particular 5109 neoprene. However, the same approach should be fruitful for other elastomers.

Even though at present the methods used in this work give only a qualitative picture of what goes on, such a picture can be of value in judging the effects of variations in formulation and processing conditions on the dispersion of carbon filler. Correlations between carbon dispersion determined this way and mechanical properties that presumably also depend upon carbon dispersion might prove useful in a practical way even in the absence of a sound theoretical connection between experimental results and underlying details of the processes.

Little emphasis has been placed upon the extraordinarily high dielectric permittivities exhibited at low to intermediate frequencies by some of these materials. These may have some practical applications as dielectrics, especially if they can be applied in the form of thin coatings to metals.

In the present study, pains were taken to keep applied fields small to avoid complications due to nonlinear effects. Such effects were noticed at fields above a few volts per centimeter, but were not further investigated. In addition, electrical properties in heavily filled materials were somewhat dependent upon sample thickness, an effect also found by others in semiconductors exhibiting dispersive transport [12]. This feature, too, was noted but not explored. Thompson et al. [33, 33a] has shown that the dc conductivity of carbon-filled 5109 neoprenes depends rather strongly upon pressure, presumably through its effect on conduction between carbon particles in clusters, and this observation offers further possibilities for study of dispersive transport in these materials.

These points are mentioned to show that much remains to be discovered and explained about carbon filled elastomers which have shown themselves to be much more puzzling and interesting dielectric materials than hitherto suspected.

ACKNOWLEDGEMENTS

It is with considerable gratitude and pleasure that I acknowledge the helpfulness of Dr. Pieter S. Dubbelday through his many stimulating and enlightening critical discussions of various phases of this lengthy investigation, and the support of Dr. Robert Y. Ting whose unflagging interest made the work possible. I wish also to express my appreciation to Drs. Corley M. Thompson and Rodger N. Capps for their helpful discussions of several phases of the work, and to Mr. Joe Morales and Ms. Linda Beumel for preparation of the special elastomer samples used in this work.

REFERENCES

1. N.G. McCrum, B.E. Read, and G. Williams, *Anelastic and Dielectric Effects in Polymeric Solids* (John Wiley & Sons, New York, 1967).
2. T.M. Birshtein, and O.B. Ptitsyn, *Conformations of Macromolecules* (Wiley Interscience, New York, 1966).
3. M.V. Volkenstein, *Configurational Statistics of Polymeric Chains* (Wiley Interscience, New York, 1963).
4. P. Hedvig, *Dielectric Spectroscopy of Polymers* (John Wiley (Halsted), New York, 1977).
5. I.I. Perepechko, *Introduction to Polymer Physics* (MIR Publishers, Moscow, 1981).
6. C.J.F. Böttcher, and P. Bordewijk, *Theory of Electric Polarization*, 2nd ed. (Elsevier, Amsterdam, 1978), Vol. II.
7. J.C. Maxwell, *A Treatise on Electricity and Magnetism* (Clarendon Press, Oxford, 1892) (also in modern Dover Edition).
8. K.W. Wagner, *Archiv für Elektrotechnik* 2, 371 (1914).
9. R.W. Sillars, "The Properties of a Dielectric Containing Semiconducting Particles of Various Shapes," *J. Inst. Elect. Engrs.* 80, 378 (1937).
10. P. Debye, *Polar Molecules* (Chem. Catalog, New York (1929) [also Dover, N.Y.], 1945).
11. H. Fröhlich, *Theory of Dielectrics* (Clarendon, Oxford, 1949).
12. H. Scher, M.F. Schlesinger, and J.T. Bendler, "Time Scale Invariance in Transport and Relaxation," *Physics Today*, pp 26-34, (1991).
13. K.L. Ngai, "Evidences for Universal Behaviour of Condensed Matter at Low Frequencies/Long Times," in *Non-Debye Relaxation in Condensed Matter* (Proceedings of a Discussion Meeting, Bangalore, ed. by T.V. Ramakrishnan and M. Raj Lakshmi, World Scientific Publishers, Singapore, 1989).
14. Yu. N. Rabotnov, *Elements of Hereditary Solid Mechanics* (Mir Publ., Moscow, 1980).

15. R.M. Christensen, *Theory of Viscoelasticity* (Academic Press, N.Y., 1971).
16. B.D. Coleman, "Thermodynamics of Materials with Memory," *Arch. Ration. Mech. Anal.* 17, 1 (1964).
17. N.A. Goryunova, *Chemistry of Diamond-Like Semiconductors* (Freeman, San Francisco, 1965), p.115.
18. W.A. Yager, "The Distribution of Relaxation Times in Typical Dielectrics," *Physics* 7, 434 (1936).
19. G.A. Niklasson, "Comparison of Dielectric Response Functions for Conducting Materials," *J. Appl. Phys.* 66, 4350 (1989).
20. M.F. Schlesinger, "Fractal Time in Condensed Matter," *Ann. Rev. Phys. Chem.* 39, 269 (1988).
21. H. Scher, and E.W. Montroll, "Anomalous Transit-time Dispersion in Amorphous Solids," *Phys. Rev. B* 12, 2455.
22. G. Williams, and D.C. Watts, "Multiple Dielectric Relaxation Processes in Amorphous Polymers as a Function of Frequency, Temperature, and Applied Pressure," in *Dielectric Properties of Polymers*, ed. by F.E. Karasz (Plenum Press, New York, 1972).
23. H. Kliem, "A Comment on Dielectric Theory; Differential Equations: Permittivity," *J. Appl. Phys.* 70, 1 (1991).
24. L.K.H. Van Beek, "Dielectric Behaviour of Heterogeneous Systems," in *Progress in Dielectrics*, Vol. 7, ed. by J.B. Birks (Heywood, London, 1967), pp. 69-114.
25. D. Polder, and J.H. Van Santen, "The Effective Permeability of Mixtures of Solids," *Physica* 12, 257 (1946).
26. C. Kittel, *Introduction to Solid State Physics*, 5th Ed. (John Wiley & Sons, New York, 1976) Ch. 10.
27. N.W. Ashcroft and N.D. Mermin, *Solid State Physics* (Holt, Rinehart, and Winston, New York, 1976), Chs. 17, 26 and 27.

28. A.K. Rajagopal and K.L. Ngai, *Relaxations in Complex Systems*, Ed. by Ngai and Wright (Naval Research Laboratory, Washington, D.C. , 1984).
29. R.W. Rendell and K.L. Ngai, "A Fundamental Relation Between Microscopic and Macroscopic Relaxation Times: Evidence in Relaxation Data," in *Relaxations in Complex Systems*, ed. by K.L. Ngai and G.B. Wright, (Naval Research Laboratory, Washington, D.C., 1984).
30. A.K. Jonscher, *Dielectric Relaxation in Solids* (Chelsea Dielectrics Press, London, 1983).
31. C.T. Moynihan, L.P. Boesch, and N.L. Laberge, "Decay Function of the Electric Field Relaxation in Vitreous Ionic Conductors," *Phys. and Chem. of Glasses* 14, 122.21. (1973).
32. L.C. Andrews and B.K. Shivamoggi, *Integral Transforms for Engineers and Applied Mathematicians* (Macmillan, New York, 1988), p. 211.
33. C.M. Thompson, T.W. Besuden, and L.L. Beumel, "Resistivity of Rubber as a Function of Mold Pressure," *Rubber Chemistry and Technology* 61, 828 (1988).
- 33a. C.M. Thompson and L.L. Beumel, "A Neoprene with Optimized Bondability for Sonar Transducer Applications," NRL Memorandum Report 5818, 1987.
34. J. Burns, P.S. Dubbelday, and R.Y. Ting, "Dynamic Bulk Modulus of Various Elastomers," *J. Polymer Sci.* B28, 1187 (1990).
35. P.S. Dubbelday and J. Burns, "Dynamic Bulk Modulus of Soft Polymers," *J. Wave-Material Interaction* 5&6, 181 (1991).
36. B.V. Hamon, "An approximate Method for Deducing Dielectric Loss Factor from Direct-Current Measurements," *Proc. Inst. Elec. Engrs.* 99, Pt. IV, Monograph 27, 151 (1952).
37. R. Zallen, *The Physics of Amorphous Solids* (Wiley-Interscience, New York, 1983).
38. J.M. Ziman, *Models of Disorder* (Cambridge University Press, London, 1979).

Appendix

5109-SERIES RUBBER FORMULATION

Basic formula:

<u>Material</u>	<u>Parts</u>
Neoprene GRT	100.0
Zinc Oxide	5.0
Octamine	2.0
90% Red Lead	15.0
TE-70	2.0
Stearic acid	1.0
Altax	1.5

To the above base mixture is added the following parts of N550 carbon black to make up the designated 5109 rubber:

<u>5109-series designation</u>	<u>Parts N550</u>	<u>Wgt. % carbon black</u>
5109-G	0	0
5109-S4	11	8.0
5109-S3	18	12.5
5109-S	31	19.7
5109-S/2	36	22.2
5109	40	24.0
5109-H	45	26.2
5109-SH	60	32.3

Note: Many of the mechanical and electrical properties of these filled elastomers depend sensitively upon details of the preparation such as time, temperature, and pressure in addition to their material formulation. Thus, some properties reported in this memorandum may differ from those reported elsewhere on what appears, from just the basic chemical formulation, to be the same elastomer. Great care was taken in preparing the series of samples used in this work to standardize the preparation. Comparisons of dielectric measurements made on different batches of the same sample designation, e.g., 5109S, differed by only a few percent.